

# CDNF rescues motor neurons in models of amyotrophic lateral sclerosis by targeting endoplasmic reticulum stress

Francesca De Lorenzo,<sup>1,2</sup> Patrick Lüningschrör,<sup>3</sup> Jinhan Nam,<sup>1,2</sup> Liam Beckett,<sup>1,2</sup> Federica Pilotto,<sup>4</sup> Emilia Galli,<sup>1</sup> Päivi Lindholm,<sup>1</sup> Cora Rüdts von Collenberg,<sup>3</sup> Simon Tii Mungwa,<sup>3</sup> Sibylle Jablonka,<sup>3</sup> Julia Kauder,<sup>5</sup> Nadine Thau-Habermann,<sup>5</sup> Susanne Petri,<sup>5</sup> Dan Lindholm,<sup>6,7</sup> Smita Saxena,<sup>4</sup> Michael Sendtner,<sup>3</sup> Mart Saarma<sup>1,†</sup> and Merja H. Voutilainen<sup>1,2,†</sup>

<sup>†</sup>These authors contributed equally to this work.

## Abstract

Amyotrophic lateral sclerosis is a progressive neurodegenerative disease that affects motor neurons (MNs) in the spinal cord, brainstem, and motor cortex, leading to paralysis and eventually to death within 3 to 5 years of symptom onset. To date, no cure or effective therapy is available. The role of chronic endoplasmic reticulum (ER) stress in the pathophysiology of amyotrophic lateral sclerosis, as well as a potential drug target, has received increasing attention.

Here, we investigated the mode of action and therapeutic effect of the ER-resident protein cerebral dopamine neurotrophic factor (CDNF) in three preclinical models of amyotrophic lateral sclerosis, exhibiting different disease development and etiology: (i) the conditional choline acetyltransferase (ChAT)-tTA/TRE-hTDP43-M337V rat model previously described, (ii) the widely used SOD1-G93A mouse model, and (iii) a novel slow-progressive TDP43-M337V mouse model. To specifically analyse the ER stress response in MNs, we used three main methods: (i) primary culture of MNs derived from E13 days embryos, (ii) immunohistochemical analyses of spinal cord sections with ChAT as spinal MNs marker, and (iii) qPCR analyses of lumbar MNs isolated via laser microdissection.

We show that intracerebroventricular administration of CDFN significantly halts the progression of the disease and improves motor behavior in TDP43-M337V and SOD1-G93A rodent models of amyotrophic lateral sclerosis. CDFN rescues motor neurons *in vitro* and *in vivo* from ER stress-associated cell death and its beneficial effect is independent of genetic disease etiology.

Notably, CDFN regulates the unfolded protein response (UPR) initiated by transducers IRE1 $\alpha$ , PERK, and ATF6, thereby enhancing MN survival.

Thus, CDFN holds great promise for the design of new rational treatments for amyotrophic lateral sclerosis.

**Author affiliations:**

1 Institute of Biotechnology, HiLIFE, P.O. Box 56, Viikki Biocenter 2, University of Helsinki, FIN-00014, Helsinki, Finland

2 Division of Pharmacology and Drug therapy, Faculty of Pharmacy, P.O. Box 56, Viikki Biocenter 2, University of Helsinki, FIN-00014, Helsinki, Finland

3 Institute of Clinical Neurobiology, University Hospital Würzburg, 97078 Würzburg, Germany

4 Department of Neurology, Inselspital University Hospital, University of Bern, CH-3010 Bern, Switzerland

5 Department of Neurology, Hannover Medical School, 30625 Hannover, Germany

6 Medicum, Department of Biochemistry and Developmental Biology, Faculty of Medicine, University of Helsinki, Helsinki, Finland

7 Minerva Foundation Institute for Medical Research, Helsinki, Finland

Correspondence to: Merja Voutilainen

Division of Pharmacology and Drug therapy, Faculty of Pharmacy, P.O. Box 56, Viikki Biocenter 2, University of Helsinki, FIN-00014, Helsinki, Finland

E-mail: merja.h.voutilainen@helsinki.fi

**Running title:** CDFN rescues MNs by targeting ER stress

**Keywords:** CDFN; ER stress; amyotrophic lateral sclerosis; unfolded protein response; motor neurons

**Abbreviations:** ABC = avidin-biotin complex; ATF6 = activating transcription factor 6; BDNF = brain-derived neurotrophic factor; CDNF = cerebral dopamine neurotrophic factor; ChAT = choline acetyltransferase; CNTF = ciliary neurotrophic factor; C9orf72 = chromosome 9 open reading frame 72; DAB = 3'-diaminobenzidine; ER = endoplasmic reticulum; HRP = horseradish peroxidase; i.c.v. = intracerebroventricular; iPSC = induced pluripotent stem cells; IRE1 = inositol-requiring enzyme 1; MANF = mesencephalic astrocyte-derived neurotrophic factor; MN = motor neuron; PDI = protein disulfide isomerase; PERK = protein kinase RNA-like endoplasmic reticulum kinase; SOD1 = superoxide dismutase 1; TDP43 = TAR DNA-binding protein 43; TM = tunicamycin; TP = thapsigargin; UPR = unfolded protein response; UT = untreated; WT = wild type

## Introduction

Amyotrophic lateral sclerosis is a progressive motor disorder characterized by the dysfunction and death of motor neurons (MNs) in the spinal cord, brainstem, and motor cortex, which results in the atrophy of skeletal muscles and paralysis. Any cure or disease-modifying therapy is currently lacking. Amyotrophic lateral sclerosis patients die within 3 to 5 years of diagnosis and respiratory failure is the most common cause of death.<sup>1</sup> To date, the etiology of amyotrophic lateral sclerosis remains mostly unknown: only about 5-10% of the cases are familial, while the remaining 90-95% of the cases occur sporadically, indicating the influence of multiple factors in its pathogenesis. Accumulation of misfolded and aggregated proteins leads to endoplasmic reticulum (ER) stress, which eventually activates the unfolded protein response (UPR). The UPR is a physiological signaling cascade that suppresses protein translation, degrades misfolded proteins, and facilitates protein folding. In mammalian cells, the UPR consists of three pathways, initiated by transmembrane ER sensors at the ER membrane: inositol-requiring enzyme 1 (IRE1), protein kinase RNA-like endoplasmic reticulum kinase (PERK), and activating transcription factor 6 (ATF6). At onset, the UPR is protective, but, under prolonged ER stress conditions, the UPR promotes apoptotic pathways.<sup>2</sup>

Substantial evidence supports the involvement of chronic ER stress in the pathophysiology of MN degeneration in amyotrophic lateral sclerosis, both in patients and animal models. UPR

markers were found to be upregulated in the spinal cord of sporadic and familial amyotrophic lateral sclerosis patients<sup>3-6</sup> and increased amount of protein disulfide isomerase (PDI) was detected in the cerebrospinal fluid of sporadic patients.<sup>3</sup> Transcriptional analysis of MNs derived from induced pluripotent stem cells (iPSCs) of patients revealed that UPR alterations were conserved among MNs harbouring SOD1 or C9ORF72 mutations, emphasizing the susceptibility of MNs to ER stress.<sup>7-9</sup>

Fast-fatigable MNs in the SOD1 transgenic mice were shown to be intrinsically more sensitive to ER stress<sup>10</sup> and an analogous upregulation of UPR markers was also reported in other studies on this mouse model.<sup>11,12</sup> Interestingly, a recent work revealed that, under chronic ER stress conditions, also wild type (WT) SOD1 protein tends to aggregate in mice, forming abnormal species.<sup>13</sup> Similarly, pharmacological induction of ER stress causes TDP43 to accumulate and, *vice versa*, overexpression of mutated TDP43 triggers ER stress.<sup>14</sup> Genetic ablation of the ER chaperone SIL-1 in the SOD1-G93A mouse model enhanced ER stress and consequently exacerbated the disease progression, emphasizing the importance of ER homeostasis in amyotrophic lateral sclerosis pathophysiology.<sup>15</sup> Furthermore, translocation of FUS protein from the nucleus to the cytoplasm has been linked to ER stress.<sup>16,17</sup>

Additionally, mutations in genes encoding ER proteins have been linked to familial and sporadic cases of amyotrophic lateral sclerosis. A missense mutation E102Q in the ER chaperone Sigma-1 receptor gene has been reported in a few familial cases.<sup>18</sup> A total of nine PDIA1 missense variants and seven PDIA3 missense variants for the gene encoding PDI were identified in sporadic patients.<sup>19</sup>

Compounds interfering specifically with the PERK/p-eIF2alpha pathway or the knockdown of its downstream effector ATF4 partially alleviate the disease phenotype in the SOD1-G93A rodent model, providing neuroprotection and delaying disease progression.<sup>10,20-22</sup> Inhibiting the IRE1 $\alpha$  - XBP1 arm of UPR signalling since embryonic stage revealed a beneficial role in the disease pathophysiology, due to an enhanced clearance of mutant SOD1 aggregates by autophagy pathways.<sup>4</sup> Moreover, targeting ER folding capacity and homeostasis by overexpression of SIL-1 in the SOD1-G93A mouse model proved to be neuroprotective and prolonged survival.<sup>15</sup>

Until now, only inhibitors of individual UPR pathways have been described, but due to the double-edged sword nature of UPR, molecules modulating all three pathways are needed.

Despite efforts to find drugs targeting ER stress to treat protein-misfolding and aggregation disorders, its value as a pharmacological target warrants further exploration.

Cerebral dopamine neurotrophic factor (CDNF) is an ER-resident protein expressed in the central nervous system mostly in neurons and peripheral tissues, including skeletal muscles, the target tissue of MNs.<sup>23</sup> By virtue of its C-terminal signal KTEL, which resembles the canonical Lys-Asp-Glu-Leu (KDEL) sequence for ER retention, CDNF-protein is primarily located in the ER lumen and secretion of mouse CDNF is regulated by the ER-resident proteins GRP78 and KDEL-R1.<sup>24</sup> The analysis of CDNF knockout mice, as well as closely related mesencephalic astrocyte-derived neurotrophic factor (MANF 59% sequence homology with CDNF) knockout mice, revealed an increase in the UPR response in several tissues in the absence of CDNF and/or MANF,<sup>25-27</sup> hinting to a role of CDNF in regulating the ER stress response. When overexpressed or microinjected into neurons, CDNF rescues cells from ER stress-induced apoptosis.<sup>23</sup> In a recent paper from our group, we showed that deleting the ER retention signal KTEL significantly reduced the neuroprotective effect of CDNF, suggesting that a reduced ER localization caused a loss in the anti-apoptotic activity of CDNF.<sup>28</sup> CDNF's ability to rescue neurons from apoptosis was also blocked by IRE1a and PERK inhibitors. CDNF protects and restores dopamine neurons in rodent and non-human primate models of Parkinson's disease.<sup>23,29-31</sup> CDNF was tested in Phase I-II trial on Parkinson's patients and the study met primary endpoints of safety and tolerability at 12 months (Clinical trial number NCT03295786).<sup>32</sup>

In order to determine the efficacy and potential of CDNF as a drug candidate for amyotrophic lateral sclerosis, we treated three independent rodent models: (i) a severe fast progressing TDP43- M337V rat model of acute induction of TDP-43-M337V toxicity, previously described by Huang *et al.*<sup>33</sup>; (ii) the well-characterized SOD1-G93A mouse model; (iii) a novel chronic TDP43-M337V expressing mouse model. Albeit being very different from each other, all three models exhibited signs of ER stress and death of MNs. Our results reveal that CDNF markedly delays the pathological phenotype and rescues MNs from ER stress-induced cell death in all three models, indicating that ER stress is an important component of the pathophysiology of amyotrophic lateral sclerosis, irrespective of its genetic etiology. Moreover, our data provide evidence that CDNF-mediated inhibition of ER stress at diseases stages has potential as a therapeutic intervention for this disorder.

## Materials and methods

### Study design

Being aware of the drawbacks of available amyotrophic lateral sclerosis pre-clinical models, we used three different models: (i) the conditional choline acetyltransferase (ChAT)-tTA/TRE-hTDP43-M337V rat model described by *Huang et al.*,<sup>33</sup> (ii) the SOD1-G93A mouse model, and (iii) a slow-progressive TDP43-M337V mouse model. We monitored disease progression and evaluated motor behavior through a battery of different motor test. To evaluate the ER stress response specifically in MNs, which are the most affected cell-type in amyotrophic lateral sclerosis, we utilized three main methods: (i) primary culture of MNs derived from E13 embryos, (ii) immunohistochemical analyses of spinal cord sections with ChAT as spinal MNs marker, and (iii) qPCR analyses of lumbar MNs isolated via laser microdissection. All the specific methods and characteristics of the animal models are described in the supplementary materials.

### Data availability

All raw data are available upon request.

## Results

### CDNF treatment rescues motor neurons and improves motor behavior in a TDP43-M337V rat model

To investigate the potential neuroprotective effect of CDFN in amyotrophic lateral sclerosis, we started administering CDFN in the acute ChAT-tTA/TRE-hTDP43-M337V rat model introduced by *Huang et al.*<sup>33</sup> In this preclinical model, the expression of human mutated TDP43 protein was dependent on the choline acetyltransferase (ChAT) promoter via a Tet-regulatory system. The transgene was kept inactive until adult age by administration of doxycycline (Dox) in drinking water (50 mg/ml). At the age of 60 days, Dox was completely withdrawn from the water and expression of TDP43-M337V protein became evident in the spinal cord MNs of the rats already

three days later. In the original study, the model showed a severe disease development, as the rats exhibited signs of motor impairment within a week and reached paralysis about one week after the onset of the disease phenotype. At this stage, over 60% of spinal MNs were lost in the transgenic rats, and within 20 days all the animals had reached the end point.<sup>33</sup> As the progression of the disease was very fast and, therefore, the therapeutic window was narrow, we decided to implement the protocol and opted for a partial withdrawal of Dox, instead of a complete one. Starting from 60 days of age, rats were administrated Dox in drinking water at a concentration of 10 mg/ml (**Fig. 1A**). The partial withdrawal of Dox-induced a slower progression of the disease (**Fig. 1B**). A continuous infusion of 6 µg/day of CDNF or phosphate-buffered saline (PBS) as vehicle in the brain lateral ventricle of TDP43-M337V and WT littermates was achieved by using Alzet minipumps. The minipumps, connected through a catheter to a cannula directly infusing in the cerebral ventricle (i.c.v.), were implanted one week before the activation of the transgene and continued to administer CDNF or the vehicle for 28 days. After the partial withdrawal of Dox, the rats were monitored for weight and motor behavioral changes for three weeks (**Supplementary Fig. 1, Fig. 1B**). Upon transgene activation, no difference in the rotarod performance was detected between the TDP43-M337V rats and the tTA littermates (used as control) until day 10. The ability to run on the rotating rod decreased substantially in the transgenic rats from day 10 onwards and major signs of hind limb stiffness and gait impairment were detected by day 20 (**Fig. 1B**). A continuous i.c.v. administration of CDNF significantly ameliorated the motor performance of treated TDP43-M337V, which was comparable to tTA littermates. No difference over time in the latency to fall was detected in tTA rats (**Fig. 1B**). Moreover, we verified whether the improvement in the motor performance of CDNF treated rats compared to PBS treated ones correlated with the number of MNs in the lumbar spinal cord. Indeed, we found that the transgenic rats that received PBS lost about 50% of the lumbar spinal MNs but treatment with CDNF significantly increased the number of surviving MNs in the same area to about 75% in comparison to the tTA controls (**Fig. 1C-D**).

## CDNF attenuates the ER stress response in the TDP43-M337V *in vitro* and *in vivo*

Next, we sought to identify whether the protective effect of CDFN lay in its ability to reduce the ER stress response, as previous evidence has hinted to a possible role of CDFN in the ER homeostasis.<sup>28,34</sup> Thus, we examined the effect of CDFN *in vitro* on MNs isolated from embryonic day 13 (E13) mice. Neurons were pharmacologically stressed with thapsigargin (TP) to induce ER stress, and then treated with CDFN. 24 hours after TP treatment, the survival of MNs was reduced to about 30% and CDFN treatment was able to improve the rate of MNs survival to 60% (**Fig. 2A**). To verify whether this positive outcome was due to a specific attenuation of the UPR pathways, we extended our dataset including new treatment groups where CDFN was administrated in combination with PERK inhibitor GSK2606414, IRE1 ribonuclease (RNase) inhibitor 4 $\mu$ 8C or kinase-inhibiting RNase attenuator 6 (KIRA6). We hypothesized that inhibition of the UPR pathways would block CDFN survival-promoting activity. Three different concentrations of the inhibitors were used, and we observed that the beneficial effect of CDFN was inversely correlated with the increasing concentrations of GSK2606414, 4 $\mu$ 8C, and KIRA6. The highest concentration of each inhibitor significantly blocked CDFN action (**Fig. 2A**). Survival assays with all three inhibitors in absence of TP were also performed to exclude any potential toxic effect of the inhibitors themselves. The survival of MNs was evaluated either in the presence or absence of established neurotrophic factors BDNF<sup>35</sup> and CNTF,<sup>36</sup> which have been shown to increase MNs survival *in vitro*. Inhibiting IRE1 or PERK pathways did not have any effects on naive cells, neither beneficial nor toxic and did not influence CNTF and BDNF survival promoting effect (**Fig. 2B**). Furthermore, we analysed the effect of CDFN treatment on the modulation of each UPR pathway in TP-stressed WT TDP43 and mutated TDP43-M337V expressing neurons. To address whether CDFN acts on the IRE-1 branch of the UPR, GFP-tagged IRE-1 was expressed in MNs via lentiviral transduction and MNs were treated with TP after 5 days. As previously described, we observed a clustering of IRE1 upon ER stress induction.<sup>37</sup> Therefore, we used the number of IRE1 clusters per cell and the percentage of cells with GFP-positive clusters as a readout for IRE1 activation. We observed that some TDP43-M337V-expressing cells already showed clustering of IRE1 without TP treatment when cultured without CDFN, while in WT cells the activation of IRE1 was only detectable upon treatment



with TP. CDNF was able to reduce IRE1 clustering in all the aforementioned conditions (**Fig. 2C and E-F**). Similarly, WT and TDP43-M337V MNs were transduced with ATF6-GFP lentiviral vectors to evaluate the translocation of ATF6 protein from the cytoplasm to the nucleus of neurons. A partial translocation of ATF6 was found in both TP-treated WT and TDP43-M337V MNs and it was reduced by CDNF administration (**Fig. 2D and G**). The partial translocation of ATF6 most likely reflects the fact that only a subset of ATF6-EGFP is cleaved and translocates to the nucleus. Finally, TDP43 and mutated TDP43-M337V expressing neurons were cultured with or without CDNF and pharmacologically stressed with TP or tunicamycin (TM) to induce ER stress. The protein levels of phosphorylated eIF2 $\alpha$  (p-eIF2 $\alpha$ ) and CHOP (gene *Ddit3*), as well as the mRNA levels of *Chop*, were decreased by CDNF treatment (**Fig. 2H-K, Supplementary Fig. 2A-B**). Taken together, these data indicate that CDNF attenuates ER stress in this model. The levels of phosphorylated TDP43 and the total levels of the protein did not change upon CDNF treatment (**Supplementary Fig. 2C-D**). To further investigate the neuroprotective mechanism behind CDNF action in the ChAT-tTA/TRE-hTDP43-M337V rat model, we sacrificed the rats 21 days after the transgene activation and collected the spinal cord for immunohistochemical analyses. We found that the levels of ER chaperone GRP78 (*alias* BiP, gene *Hspa5*) and p-eIF2 $\alpha$  were upregulated in the vehicle-treated TDP43-M337V rats compared to tTA controls (**Fig. 3A-F**). This increase in the ER stress response in this model was not previously described in the literature and strengthens the hypothesis of the importance of ER stress in the pathophysiology of amyotrophic lateral sclerosis. Staining of the ER-marker GRP78 was found from the perinuclear area to the cell membrane. It has been previously shown that the ER in neurons forms a highly dynamic network that can reach out to the cell surface, entering axons and presynaptic terminals, and make direct contact with the plasma membrane.<sup>38-41</sup> This may explain while the staining for GRP78 is not restricted to the perinuclear area, as in many other cell types. Upon treatment with CDNF, the expression of GRP78 and the phosphorylation of p-eIF2 $\alpha$  were significantly reduced in the ventral horn of the lumbar spinal cord and, specifically, in the ChAT<sup>+</sup> MNs (**Fig. 3A-F**).

## A single i.c.v. CDFN injection improves survival and rescues motor neurons in SOD1-G93A mice

To determine whether the effect of CDFN would be specific only to the TDP43 model or if it could be applied to any model affected by ER stress, we treated SOD1-G93A mice with CDFN. In this well-characterized amyotrophic lateral sclerosis model, chronic ER stress response in the corresponding MNs has been previously reported.<sup>10,11</sup> To this end, we utilized a single injection of CDFN, which in Parkinson's disease animal models effectively counteracted dopamine neuron degeneration.<sup>23</sup> As proof-of-principle, we first confirmed that CDFN and <sup>125</sup>I-labelled CDFN injected in the brain lateral ventricle efficiently diffuse to different areas of the brain, including cortex, striatum, and substantia nigra, and to the lumbar spinal cord (**Supplementary Fig. 3**). Moreover, we found that CDFN specifically co-localizes with lumbar MNs (**Supplementary Fig. 4**). 13 weeks SOD1-G93A mice (early disease stage) and WT littermates of 13 weeks of age received a single i.c.v. injection of 10 µg of human CDFN or PBS as vehicle and were examined twice a week to follow changes in disease indications and motor behavior until the final stage of paralysis (experimental timeline in **Fig. 4A**). At the time of treatment, SOD1-G93A mice displayed measurable tremors in the hind limbs. Upon a single CDFN injection, SOD1-G93A mice developed gait impairment and paralysis significantly more slowly than PBS-treated mutant littermates (**Supplementary Fig. 5A-B**), and, in females but not in males, we also observed a slower decrease in body weight (**Supplementary Fig. 5C-D**). The median survival time in females was 148 days for CDFN-treated mice and 140 days for PBS-treated mice, with an increase of 8 days. In males, the median survival was 140.5 days for the CDFN-treated mice and 132 days for the PBS-treated mice, with an increase of 8.5 days (**Fig. 4B-C**). Along with this, their balance and motor behavior performance were significantly ameliorated by CDFN treatment. In the accelerating rotarod, CDFN-treated female and male mice showed an increased latency to fall compared to vehicle-treated mice. No statistical differences were found in CDFN or vehicle-injected WT littermates over time (**Fig. 4D-E**). One week after CDFN or PBS injection, the CDFN group showed an increased ability to run on the smallest 8 mm rod in the multiple static rods experimental paradigm for females and on the 21 and 11 mm rods for males (**Fig. 4F-G**), compared to the PBS group. These sex differences in the experimental tasks are in accordance with previous observations that males develop a major

disease phenotype approximately one week earlier than female littermates.<sup>42,43</sup> In the open field, SOD1-G93A mice exhibited fewer rearings compared to WT mice, which is associated with less strength in the hind limb muscles, and CDFN treatment increased the number of rearings compared to PBS controls at 16 weeks (**Fig. 4H**). Moreover, immunohistochemical analyses of the lumbar spinal cord revealed a significantly higher number of MNs present in the CDFN-treated compared to PBS-treated mice, which correlated with the behavioral improvement (**Fig. 4I and Supplementary Fig. 6**).

### **CDNF increases survival of SOD1-G93A embryonic motor neurons by regulating all three UPR pathways**

We further investigated whether CDFN modulates ER stress and survival of SOD1-G93A-derived embryonic MNs *in vitro* and whether its effect is limited to only one branch of the UPR or is extended to all three as in the TDP43-M337V expressing MNs. MNs from E13 WT and SOD1-G93A mouse embryos, which depend on trophic support for their survival *in vitro*, were cultured either in the presence of BDNF or CNTF or only with CDFN. Interestingly, CDFN alone had a significant effect on the survival of the MNs as compared to the untreated conditions, though not to the same degree as observed with the combination of BDNF and CNTF (**Fig. 5A**). No difference in the morphology of cultured MNs was observed between any of the aforementioned culture conditions (**Supplementary Fig. 7**). SOD1-G93A mutant MNs were obtained from the same SOD1-G93A mouse model used in the *in vivo* study, which develops first signs of a pathological phenotype at about three months after birth. However, when ER stress was induced in cultured MNs by TP treatment, these embryonic SOD1-G93A mutant MNs appeared significantly more sensitive compared to MNs from WT littermates, supporting previous observations made with this mouse model.<sup>10</sup> This sensitivity was seen despite the continuous presence of BDNF and CNTF in culture, but when CDFN was added to ER stressed SOD1-G93A mutant MNs, survival was rescued to the levels observed in WT MNs (**Fig. 5B**). The protective effect of CDFN in SOD1-G93A MNs from TP-induced ER-stress occurred in a dose-dependent manner and at a concentration of 20 ng/ml or higher the survival of SOD1-G93A MNs was comparable to that of WT cells (**Fig. 5C**). Next, we analysed whether CDFN, when compared to BDNF/CNTF, can modulate the signaling pathways of the UPR in cultured MNs treated with either TP or TM. We observed a partial translocation of ATF6 protein from the

cytoplasm to the nucleus of the neurons upon treatment with TP or TM. However, the addition of CDNF significantly reduced ATF6 translocation in SOD1-G93A treated with TP or TM (**Fig. 5D-E**). Furthermore, CDNF diminished the splicing levels of *xbp1s* transcripts observed after TP or TM treatment, particularly in SOD1-G93A MNs, suggesting an inhibition of the IRE1 $\alpha$ -linked pathway (**Fig. 5F**). Additionally, CDNF treatment significantly decreased p-eIF2 $\alpha$  and CHOP, activated downstream of the PERK signaling pathway, in TP and in TM treated SOD1-G93A MNs (**Fig. 5G-I, Supplementary Fig. 8**). Collectively, these results show that SOD1-G93A MNs are already at embryonic stage intrinsically more sensitive to ER stress and that CDNF efficiently counteracts the ER stress-induced cell death by reducing the activity of all three major UPR signaling pathways.

### **CDNF attenuates all three UPR branches initiated by PERK, IRE1 $\alpha$ , and ATF6 *in vivo***

To investigate the mechanisms involved in the *in vivo* action of CDNF in the SOD1-G93A model, we analysed the UPR signaling pathways in lumbar MNs isolated via laser microdissection (**Fig. 6A**) at 13 and 17 weeks, i.e. 5 days after CDNF i.c.v. injections (**Fig. 6B-F**). RNA was isolated from micro-dissected neurons and the mRNA levels of UPR markers were analysed. Interestingly, at 13 weeks we only found an upregulation of *Atf4* and *Chop* transcripts in PBS-treated SOD1-G93A mice compared to PBS-treated WT littermates (significance marked with # in **Fig. 6B-F**). As both molecules are downstream effectors of the PERK pathway, which blocks general protein translation initiation in stressed cells, these data suggest that this branch of UPR signaling is the first to be activated in lumbar MNs of SOD1-G93A mice. Notably, upon CDNF treatment, *Atf4* mRNA was decreased to WT levels (**Fig. 6C**). In accordance with previous results,<sup>10,11,44</sup> at 17 weeks of age the PERK, IRE-1 $\alpha$ , and ATF6 pathways were all upregulated in SOD1-G93A mice compared to WT littermates, and in particular the mRNA levels of *Chop*, which has a prominent role in apoptosis, increased more than 4-fold. CDNF treatment was able to attenuate markers from all three UPR branches (**Fig. 6B-F**). Furthermore, fluorescence staining revealed that the levels of the ER chaperone GRP78 and the phosphorylation of eIF2 $\alpha$  were increased in lumbar MNs of 17 weeks old SOD1-G93A mice, but these were efficiently reduced by CDNF administration, resulting in expression levels comparable to WT mice (**Fig. 6G-J**). Finally, we investigated whether CDNF treatment would

affect the levels of mutant SOD1 protein and its clearance using its conformation-specific antibody B8H10 (MM070, Medimabs, Canada): a trend in the reduction of mutant SOD1 protein in CDNF-treated mice was found at 17 weeks (**Supplementary Fig. 9A-B**). We did not find any difference in mutated SOD1 between CDNF and PBS-treated mice at the transcriptional level (**Supplementary Fig. 9C**).

## **Endogenous CDNF levels change with disease progression in SOD1-G93A mice**

We next evaluated the endogenous levels of CDNF in non-treated WT and SOD1-G93A mice at different disease stages, from the pre-pathological stage of 1 month to the endpoint of approximately 5 months, collected lumbar spinal cord, motor cortex, and skeletal gastrocnemius muscle samples and analysed protein levels by ELISA and mRNA levels by qPCR. We found that levels of CDNF change during SOD1-G93A lifespan. CDNF was upregulated before the appearance of a disease phenotype in the spinal cord and later in the motor cortex at the mRNA level. On the contrary, CDNF protein levels in skeletal muscle were significantly decreased at the onset of the disease phenotype stage and onwards (2, 3 and 5 months of age, **Supplementary Fig. 10**), which might correlate with reduced activity of paralyzed muscles.

## **CDNF reduces the UPR response in a slow progressive TDP43-M337V mouse model before disease onset**

Since enhanced sensitivity to ER stress in SOD1-G93A MNs is detectable starting from embryonic stages (**Fig. 5B**) and long before the appearance of first impairment signs in the corresponding mouse model (**Fig. 4**), we sought to explore the protective effect of CDNF in a third and new model of amyotrophic lateral sclerosis, which displayed a slow progressive development of the disease. In this newly generated transgenic mouse model, the murine Tdp43-M337V coding sequence N-terminally tagged to HA was expressed under the control of the human Ubiquitin C promoter (**Supplementary Fig. 11**). Staining with an HA antibody confirmed the expression of the transgene in every cell type within the spinal cord, including MNs, as shown by co-staining against ChAT (**Supplementary Fig. 11A-B**). We did not detect any TDP43 positive inclusions in these mice nor c-terminal cleavage products (**Supplementary Fig. 11B, F**). Transgenic animals were born without any obvious phenotype, but showed a

progressive, late-onset MNs loss, as determined by Nissl staining of lumbar spinal cord sections (**Supplementary Fig. 11C-D**). On the transcriptional level, we did not detect any silencing of the endogenous TDP43 (**Supplementary Fig. 11E-F**), most likely due to the mild expression of the transgene (**Supplementary Fig. 11E-F**). Aged mice showed a remodeling towards reduced number of motor units, as demonstrated by elevated amplitude of single motor unit potentials (**Supplementary Fig. 11G**). When challenged on a rocking and accelerating rotarod, we also observed an impaired motor performance in aged transgenic mice (**Supplementary Fig. 11H**). In contrast to previous reported TDP43 models with overexpression of the transgene,<sup>45,46</sup> this newly generated mouse model showed a moderate expression of the transgene, as shown by Western blot analysis (**Sup. Fig. 11E-F**). This is in agreement with two recent studies, describing the phenotype of new mouse models in which the mutation in the TDP43 gene was introduced into the endogenous locus and where only a mild motor phenotype with late onset was observed.<sup>47,48</sup> Signs of an enhanced ER stress were present long before an altered behavior was detected in this mouse model (**Fig. 7A**). To test the effect of CDNF, TDP43-M337V mice received a single i.c.v. injection of 10 µg of CDNF at 6 weeks of age and the ER stress response was analysed at 6 months of age in the spinal cord and the motor cortex of the mice (**Fig. 7B**). An exacerbation of the UPR response was found in the transgenic mice compared to the WT littermates. As expected, this upregulation was not as strong as the one detected in the SOD1-G93A at late-stage. However, treatment with CDNF had a similar effect in reducing the ER stress response, with a significant decrease in *Chop* and *Xbp1t* mRNA and an equivalent trend in most of the other genes (**Fig. 7C-H**). Moreover, the mRNA levels of the UPR markers were downregulated in the full lysate of motor cortex upon treatment with CDNF (**Fig. 7I**). Finally, we wanted to evaluate whether CDNF can improve the motor behavior and the number of surviving lumbar MNs in aged TDP43-M337V mice. Therefore, we injected 10 µg of CDNF or vehicle i.c.v. to 18 months old TDP43-M337V and age-matched WT controls. The mice were followed for 5 weeks, and weight changes and motor performance were analysed weekly (experimental timeline in **Fig. 8A**). While no significance difference in weight changes was observed (**Supplementary Fig. 12**), TDP43-M337V mice were performing worse on the rotarod compared to WT mice when challenged by rocking and reverse acceleration (**Fig. 8B-E**). CDNF-treated female TDP43-M337V mice were significantly performing better at 2, 3 and 4 weeks upon the drug administration, while an amelioration of the motor behavior in male TDP43-M337V mice was

observed at 2 and 5 weeks after injection (**Fig. 8D-E**). No difference in WT mice was found upon CDNF or PBS treatment (**Fig. 8B-C**). It should be noticed that male mice performed overall worse than female mice due to their higher weight (**Fig. 8B-E**). The mice were sacrificed 5 weeks after CDNF/vehicle injection and the number of lumbar MNs was assessed. We observed a reduced number of MNs in the spinal cord of TDP43-M337V mice compared to WT mice, but CDNF administration increased the number of surviving MNs (**Fig. 8F-G**). These results are in line with the effects observed in the TDP43-M337V rat and in the SOD1-G93A mouse and demonstrate that CDNF improves MNs survival and actively suppresses ER stress in amyotrophic lateral sclerosis preclinical models independently of the disease etiology.

## Discussion

Amyotrophic lateral sclerosis is a complex and multifactorial disease.<sup>49,50</sup> Several studies have indicated that ER stress plays a pivotal role in the pathophysiology of the disease,<sup>3-19</sup> thus it became an interesting target for therapeutic intervention. In this study, we explored the role of CDNF as a modulator of the ER stress response in amyotrophic lateral sclerosis and show that CDNF is the first compound that can attenuate all the three UPR pathways activated by IRE1 $\alpha$ , PERK, and ATF6 in MNs *in vitro* and *in vivo*. Moreover, we present evidence that the activity of IRE1 $\alpha$  and PERK pathways are required for the antiapoptotic effect of CDNF in MNs. This is remarkable, as previous compounds have been shown to interfere only with the PERK/p-eIF2 $\alpha$  pathway, in particular inhibiting the de-phosphorylation of eIF2 $\alpha$ <sup>10,20,21</sup> or by suppressing the activity of the dual leucine zipper kinase (DLK).<sup>51</sup> Small molecule allosteric inhibitors for IRE1 $\alpha$  oligomerization, KIRAs, have also been described: KIRA6 is a specific IRE-1 $\alpha$  kinase inhibitor, whereas KIRA8 blocks IRE-1 $\alpha$  RNase activity. They have been shown to reduce beta-cell ER stress and death, and thus ameliorate diabetes in mouse models.<sup>52,53</sup> We have previously discussed that all three pathways are chronically active in amyotrophic lateral sclerosis and that the UPR is a finely intertwined network. Thus, targeting only one of the pathways is not sufficient and limits the efficacy of these compounds, whereas CDNF has a broader therapeutic scope than any single pathway-specific inhibitor. Furthermore, it has also been reported that persistent translation inhibition by p-eIF2 $\alpha$ , which is accentuated by drugs as salubrinal, mediates neurodegeneration in a model of prion disease, which is another protein misfolding

disorder that shares several pathogenic mechanisms with amyotrophic lateral sclerosis.<sup>54</sup> Treatment with guanabenz, which was shown to be protective in female SOD1-G93A mice by Jiang *et al.*,<sup>21</sup> led to an opposite effect in another study, with an exacerbation of the disease phenotype especially in male mice.<sup>55</sup> These results suggest that guanabenz, especially if administered systemically, may have a detrimental effect because of a sustained block of protein translation, acceleration of apoptosis, and also because of possible side effects due to the activity of the drug as an agonist of the  $\alpha$ 2-adrenergic receptor.<sup>55</sup> On the other hand, a complete restoration of protein translation by PERK inhibitor GSK2606414, albeit being neuroprotective in a prion model, was found to be highly toxic for pancreatic cells, where UPR activation is essential for physiological activity.<sup>56</sup> These reports suggest the need for a drug candidate with the ability to attenuate the whole UPR network in affected neurons, without side effects. Interestingly, we found that CDFN has very little effect *in vitro* on healthy MNs but has a strong protective effect on injured and ER stressed-MNs. Broad toxicity assays for CDFN have been already carried out in non-human primates and CDFN was successfully tested in phase I-II clinical trial in Parkinson's disease patients.<sup>57</sup> Importantly, the long-lasting downregulation of UPR markers in the SOD1-G93A and TDP43 mouse models by CDFN, even after a single injection of CDFN, indicates that the protective effect is maintained for a long time period, highlighting its potential therapeutic value.

Chronically activated UPR pathways eventually lead to neuronal dysfunction and finally to CHOP-mediated cell death.<sup>58</sup> CDFN significantly reduced the levels of CHOP, and we postulate that CDFN inhibits CHOP-mediated apoptosis, therefore enhancing MNs survival. CDFN was also shown to activate the PI3K-Akt pathway in dopamine neurons.<sup>34</sup> In addition to the regulation of ER stress and UPR and anti-apoptotic activity, CDFN may have some other interesting properties. Analyzing the phenotype of CDFN-deficient mice we found that an age-dependent loss of enteric neurons occurs selectively in the submucosal but not in the myenteric plexus. This neuronal loss is a consequence not of increased apoptosis but of neurodegeneration and autophagy, suggesting a role for CDFN in the regulation of autophagy.<sup>59</sup> Autophagy has lately emerged as an essential protective mechanism during ER stress. These two organelle systems are dynamically interconnected, and several studies have established that ER stress can either stimulate or inhibit autophagy. In fact, the signaling pathways mediated via IRE1 $\alpha$ , PERK, ATF6, and Ca<sup>2+</sup> are necessary for the activation of ER stress-mediated autophagy.<sup>60,61</sup>



Moreover, our data on reduced mutated SOD1-G93A at the protein, but not mRNA level, suggest that the decrease may be the effect of improved clearance of the mutated protein. Therefore, previous and current results do not exclude the possibility that CDFN may exert its protective effect through other pathways in addition to the regulation of the chronic ER stress response, such as autophagy, activation of pro-survival pathways, or preventing the synthesis and release of pro-inflammatory cytokines.<sup>62</sup> These aspects should be further explored also in the context of MNs and amyotrophic lateral sclerosis disease.

The direct mechanism of action of CDFN in reducing the ER stress response is still under investigation. We have previously shown that CDFN can interact with the main ER chaperon GRP78.<sup>28</sup> In the current study we have shown that IRE1a and PERK inhibitors block CDFN ability to promote the survival of MNs, but do not inhibit the action of BDNF or CNTF. These data strongly suggest that the activity of PERK and IRE1 $\alpha$  pathways is essential for the survival-promoting activity of CDFN. Whether CDFN directly interacts with PERK and IRE1a or this interaction is facilitated by GRP78 is still unclear. It was recently discovered that MANF reduces the UPR signaling by decreasing IRE1 $\alpha$  oligomerization and IRE1 $\alpha$  phosphorylation. MANF also interacts with other UPR receptors PERK and ATF6, but with lower affinity.<sup>63</sup> In the light of these results, we favor the hypothesis that CDFN may directly interact with the UPR sensors PERK and IRE1a. These problems require, however, a thorough independent investigation.

Due to the genetically variegated and multifactorial nature of amyotrophic lateral sclerosis, creating an animal model that would properly mimic all the pathophysiological events involved in the development and progression of the disease has revealed as a complex task.<sup>64</sup> Therefore, being aware of the advantages and disadvantages of available pre-clinical model, we sought to investigate the therapeutic effect of CDFN and in three rodent models with different etiology and disease development, harboring mutations in either SOD1 or TDP43. Albeit their differences, all three models exhibit signs of ER stress and death of MNs. Accumulation of misfolded/unfolded proteins in the ER lumen is one determinant for the initiation of the ER stress; however, ER stress, and consequent UPR, is induced by a plethora of other stressors, including calcium buffering, inflammation, proteostasis impairment, altered neuronal activity, mitochondrial dysfunction, aging, etc. Notably, ER stress can be triggered by depletion of ER calcium, and impaired calcium homeostasis has been well documented in most familial forms of amyotrophic lateral sclerosis.<sup>65-67</sup> Mutated SOD1-G93A and TDP43, albeit being mostly found in the

cytoplasm, interfere with some of these processes. As an example, mutant SOD1 protein has been shown to be a strong inducer of the ubiquitin-proteasome system (UPS).<sup>12,68</sup> In addition, TDP43 accumulation within the rough ER membrane has been documented in amyotrophic lateral sclerosis patients.<sup>6</sup>

To implement our study on CDNF's role in the regulation of the UPR response, we used embryonic cultured MNs harboring SOD1-G93A and TDP43-M337V mutations. As there was only a modest UPR activation in untreated SOD1-G93A and TDP43-M337V MNs, we induced ER stress pharmacologically using either TP or TM. The modest UPR activation can be explained with the fact that cultured MNs are derived from embryonic mice and not adult mice. Albeit ER stress signs have been found in SOD1-G93A mice<sup>10</sup> and TDP43-M337V mice (**Fig. 7**) at a pre-symptomatic stage, these data refer to adult mice. We reckon that it will take time for the mutations to cause a chronic ER stress response, and therefore the UPR response is low at the embryonic level. Moreover, MNs cultures are highly enriched and do not contain activated microglia or immune cells, which provide pro-apoptotic stimuli and usually contribute to the pathophysiology of neurodegeneration. The reduction in the UPR response in isolated MNs demonstrate the direct effect of CDNF on MNs and exclude the possibility of indirect effect that are mediated through other cell types.

Administration of CDNF via the i.c.v. route attenuated the ER stress response, increased the number of surviving MNs and improved the motor behavior in the mouse SOD1-G93A and in both the mouse and rat TDP43-M337V models, irrespective of the disease etiology. We believe that this enhances the predictive value that CDNF could also be beneficial in patients with amyotrophic lateral sclerosis. To the best of our knowledge, no previous drug candidate has been reported to have a protective effect in this severe and fast progressive TDP43 rat model. In a recent report, it was shown that riluzole had no therapeutic efficacy on the behavioral deficits, nor on the neuropathological features in this model.<sup>69</sup> Furthermore, CDNF showed a beneficial effect in the SOD1-G93A mice when treated at 3 months of age, i.e., after disease signs onset. This is a clinically relevant time point for initiation of therapy in patients, as usually they are not diagnosed before disease onset. SOD1-G93A mice treated daily with riluzole in drinking water, starting approximately 40 days before the onset of a disease phenotype, showed improved survival by 13 days,<sup>70</sup> whereas no increase in survival was observed after edaravone intraperitoneal administration.<sup>71</sup> Additionally, the evidence from our novel TDP43-M337V

mouse model that ER stress is already present before the appearance of a pathological phenotype suggests that CDFN is also a strong candidate for the prevention of disease initiation in amyotrophic lateral sclerosis cases with familial monogenic origin.

Finally, in this study we demonstrate that endogenous levels of CDFN change during disease progression, being upregulated at pre-disease stages and decreasing at later stages. In particular, the decreased levels of CDFN in muscle compared to WT might correlate with paralysis and reduced activity of non-functional muscle. Furthermore, the decrease in the endogenous levels of CDFN with disease progression suggests that the administration of exogenous protein at this stage should have a therapeutic effect, which is supported by the results described here.

In conclusion, CDFN rescues MNs *in vitro* and *in vivo* by regulating the ER stress response, a key player in the pathophysiology of amyotrophic lateral sclerosis. Hence, we propose that CDFN is a promising ER stress regulator for injured MNs that warrants further study as a drug candidate in amyotrophic lateral sclerosis.

## Acknowledgements

Katrina Albert, Emilia Hella, Pushpa Khanal, Jaan Korpikoski, Ella Montonen, Anni Saukkonen, Matilda Sinkko and Janika Sirjala are thanked for their technical help.

## Funding

Jane and Aatos Erkko Foundation; Academy of Finland (grants ID 309708, 314233); ALS Association (grant ID: 18-IIA-422); Department of Defense (grant ID: AL160114); E-Rare ("9th Joint Call for European Research Projects on Rare Diseases, JTC 2017); Sigrid Jusélius Foundation.

## Competing interests

Päivi Lindholm, Mart Saarma and Merja H Voutilainen are inventors of the CDFN-patent, which is owned by Herantis Pharma Plc. M Saarma is a shareholder of Herantis Pharma Plc.

## Supplementary material

Supplementary material is available at *Brain* online.

## References

1. Kiernan MC, Vucic S, Cheah BC, *et al.* Amyotrophic lateral sclerosis. *Lancet*. Mar 12 2011;377(9769):942-55. doi:10.1016/s0140-6736(10)61156-7
2. Hetz C, Saxena S. ER stress and the unfolded protein response in neurodegeneration. *Nat Rev Neurol*. Aug 2017;13(8):477-491. doi:10.1038/nrneurol.2017.99
3. Atkin JD, Farg MA, Walker AK, McLean C, Tomas D, Horne MK. Endoplasmic reticulum stress and induction of the unfolded protein response in human sporadic amyotrophic lateral sclerosis. *Neurobiol Dis*. Jun 2008;30(3):400-7. doi:10.1016/j.nbd.2008.02.009
4. Hetz C, Thielen P, Matus S, *et al.* XBP-1 deficiency in the nervous system protects against amyotrophic lateral sclerosis by increasing autophagy. *Genes Dev*. Oct 1 2009;23(19):2294-306. doi:10.1101/gad.1830709
5. Ito Y, Yamada M, Tanaka H, *et al.* Involvement of CHOP, an ER-stress apoptotic mediator, in both human sporadic ALS and ALS model mice. *Neurobiol Dis*. Dec 2009;36(3):470-6. doi:10.1016/j.nbd.2009.08.013
6. Sasaki S. Endoplasmic reticulum stress in motor neurons of the spinal cord in sporadic amyotrophic lateral sclerosis. *J Neuropathol Exp Neurol*. Apr 2010;69(4):346-55. doi:10.1097/NEN.0b013e3181d44992
7. Dafinca R, Scaber J, Ababneh N, *et al.* C9orf72 Hexanucleotide Expansions Are Associated with Altered Endoplasmic Reticulum Calcium Homeostasis and Stress Granule Formation in Induced Pluripotent Stem Cell-Derived Neurons from Patients with Amyotrophic Lateral Sclerosis and Frontotemporal Dementia. *Stem Cells*. Aug 2016;34(8):2063-78. doi:10.1002/stem.2388
8. Kiskinis E, Sandoe J, Williams LA, *et al.* Pathways disrupted in human ALS motor neurons identified through genetic correction of mutant SOD1. *Cell Stem Cell*. Jun 5 2014;14(6):781-95. doi:10.1016/j.stem.2014.03.004
9. Zhang YJ, Jansen-West K, Xu YF, *et al.* Aggregation-prone c9FTD/ALS poly(GA) RAN-translated proteins cause neurotoxicity by inducing ER stress. *Acta Neuropathol*. Oct 2014;128(4):505-24. doi:10.1007/s00401-014-1336-5

10. Saxena S, Cabuy E, Caroni P. A role for motoneuron subtype-selective ER stress in disease manifestations of FALS mice. *Nat Neurosci.* May 2009;12(5):627-36. doi:10.1038/nn.2297
11. Kikuchi H, Almer G, Yamashita S, *et al.* Spinal cord endoplasmic reticulum stress associated with a microsomal accumulation of mutant superoxide dismutase-1 in an ALS model. *Proc Natl Acad Sci U S A.* Apr 11 2006;103(15):6025-30. doi:10.1073/pnas.0509227103
12. Nishitoh H, Kadowaki H, Nagai A, *et al.* ALS-linked mutant SOD1 induces ER stress- and ASK1-dependent motor neuron death by targeting Derlin-1. *Genes Dev.* Jun 1 2008;22(11):1451-64. doi:10.1101/gad.1640108
13. Medinas DB, Rozas P, Martinez Traub F, *et al.* Endoplasmic reticulum stress leads to accumulation of wild-type SOD1 aggregates associated with sporadic amyotrophic lateral sclerosis. *Proc Natl Acad Sci U S A.* Aug 7 2018;115(32):8209-8214. doi:10.1073/pnas.1801109115
14. Walker AK, Soo KY, Sundaramoorthy V, *et al.* ALS-associated TDP-43 induces endoplasmic reticulum stress, which drives cytoplasmic TDP-43 accumulation and stress granule formation. *PLoS One.* 2013;8(11):e81170. doi:10.1371/journal.pone.0081170
15. Filezac de L'Etang A, Maharjan N, Cordeiro Brana M, *et al.* Marinesco-Sjogren syndrome protein SIL1 regulates motor neuron subtype-selective ER stress in ALS. *Nat Neurosci.* Feb 2015;18(2):227-38. doi:10.1038/nn.3903
16. Farg MA, Soo KY, Walker AK, *et al.* Mutant FUS induces endoplasmic reticulum stress in amyotrophic lateral sclerosis and interacts with protein disulfide-isomerase. *Neurobiol Aging.* Dec 2012;33(12):2855-68. doi:10.1016/j.neurobiolaging.2012.02.009
17. Farg MA, Soo KY, Warraich ST, Sundaramoorthy V, Blair IP, Atkin JD. Ataxin-2 interacts with FUS and intermediate-length polyglutamine expansions enhance FUS-related pathology in amyotrophic lateral sclerosis. *Hum Mol Genet.* Feb 15 2013;22(4):717-28. doi:10.1093/hmg/ddz479
18. Couly S, Khalil B, Viguier V, Roussel J, Maurice T, Lievens JC. Sigma-1 receptor is a key genetic modulator in amyotrophic lateral sclerosis. *Hum Mol Genet.* Nov 7 2019;doi:10.1093/hmg/ddz267
19. Gonzalez-Perez P, Woehlbier U, Chian RJ, *et al.* Identification of rare protein disulfide isomerase gene variants in amyotrophic lateral sclerosis patients. *Gene.* Jul 25 2015;566(2):158-65. doi:10.1016/j.gene.2015.04.035
20. Das I, Krzyzosiak A, Schneider K, *et al.* Preventing proteostasis diseases by selective inhibition of a phosphatase regulatory subunit. *Science.* Apr 10 2015;348(6231):239-42. doi:10.1126/science.aaa4484
21. Jiang HQ, Ren M, Jiang HZ, *et al.* Guanabenz delays the onset of disease symptoms, extends lifespan, improves motor performance and attenuates motor neuron loss in the SOD1 G93A mouse model of amyotrophic lateral sclerosis. *Neuroscience.* Sep 26 2014;277:132-8. doi:10.1016/j.neuroscience.2014.03.047
22. Matus S, Lopez E, Valenzuela V, Nassif M, Hetz C. Functional contribution of the transcription factor ATF4 to the pathogenesis of amyotrophic lateral sclerosis. *PLoS One.* 2013;8(7):e66672. doi:10.1371/journal.pone.0066672
23. Lindholm P, Voutilainen MH, Lauren J, *et al.* Novel neurotrophic factor CDNF protects and rescues midbrain dopamine neurons in vivo. *Nature.* Jul 5 2007;448(7149):73-7. doi:10.1038/nature05957

24. Norisada J, Hirata Y, Amaya F, Kiuchi K, Oh-hashii K. A Comparative Analysis of the Molecular Features of MANF and CDFN. *PLoS One*. 2016;11(1):e0146923. doi:10.1371/journal.pone.0146923
25. Lindahl M, Danilova T, Palm E, *et al.* MANF is indispensable for the proliferation and survival of pancreatic beta cells. *Cell Rep*. Apr 24 2014;7(2):366-375. doi:10.1016/j.celrep.2014.03.023
26. Pakarinen E, Danilova T, Vöikar V, *et al.* MANF Ablation Causes Prolonged Activation of the UPR without Neurodegeneration in the Mouse Midbrain Dopamine System. *eNeuro*. Jan/Feb 2020;7(1)doi:10.1523/eneuro.0477-19.2019
27. Pakarinen E, Lindholm P, Saarma M, Lindahl M. CDFN and MANF regulate ER stress in a tissue-specific manner. *Cell Mol Life Sci*. Feb 7 2022;79(2):124. doi:10.1007/s00018-022-04157-w
28. Eesmaa A, Yu LY, Göös H, *et al.* CDFN Interacts with ER Chaperones and Requires UPR Sensors to Promote Neuronal Survival. *Int J Mol Sci*. Aug 22 2022;23(16)doi:10.3390/ijms23169489
29. Airavaara M, Harvey BK, Voutilainen MH, *et al.* CDFN protects the nigrostriatal dopamine system and promotes recovery after MPTP treatment in mice. *Cell Transplant*. 2012;21(6):1213-23. doi:10.3727/096368911x600948
30. Garea-Rodriguez E, Eesmaa A, Lindholm P, *et al.* Comparative Analysis of the Effects of Neurotrophic Factors CDFN and GDNF in a Nonhuman Primate Model of Parkinson's Disease. *PLoS One*. 2016;11(2):e0149776. doi:10.1371/journal.pone.0149776
31. Voutilainen MH, Back S, Peranen J, *et al.* Chronic infusion of CDFN prevents 6-OHDA-induced deficits in a rat model of Parkinson's disease. *Exp Neurol*. Mar 2011;228(1):99-108. doi:10.1016/j.expneurol.2010.12.013
32. Lindholm P, Saarma M. Cerebral dopamine neurotrophic factor protects and repairs dopamine neurons by novel mechanism. *Mol Psychiatry*. Dec 14 2021;doi:10.1038/s41380-021-01394-6
33. Huang C, Tong J, Bi F, Zhou H, Xia XG. Mutant TDP-43 in motor neurons promotes the onset and progression of ALS in rats. *J Clin Invest*. Jan 2012;122(1):107-18. doi:10.1172/jci59130
34. Voutilainen MH, De Lorenzo F, Stepanova P, *et al.* Evidence for an Additive Neurorestorative Effect of Simultaneously Administered CDFN and GDNF in Hemiparkinsonian Rats: Implications for Different Mechanism of Action. *eNeuro*. Jan-Feb 2017;4(1)doi:10.1523/eneuro.0117-16.2017
35. Yan Q, Elliott J, Snider WD. Brain-derived neurotrophic factor rescues spinal motor neurons from axotomy-induced cell death. *Nature*. Dec 24-31 1992;360(6406):753-5. doi:10.1038/360753a0
36. Sendtner M, Kreutzberg GW, Thoenen H. Ciliary neurotrophic factor prevents the degeneration of motor neurons after axotomy. *Nature*. May 31 1990;345(6274):440-1. doi:10.1038/345440a0
37. Li H, Korennykh AV, Behrman SL, Walter P. Mammalian endoplasmic reticulum stress sensor IRE1 signals by dynamic clustering. *Proc Natl Acad Sci U S A*. Sep 14 2010;107(37):16113-8. doi:10.1073/pnas.1010580107
38. Cohen S, Valm AM, Lippincott-Schwartz J. Interacting organelles. *Curr Opin Cell Biol*. Aug 2018;53:84-91. doi:10.1016/j.ceb.2018.06.003

39. Deng C, Moradi M, Reinhard S, *et al.* Dynamic remodeling of ribosomes and endoplasmic reticulum in axon terminals of motoneurons. *J Cell Sci.* Nov 15 2021;134(22)doi:10.1242/jcs.258785
40. Terasaki M, Reese TS. Interactions among endoplasmic reticulum, microtubules, and retrograde movements of the cell surface. *Cell Motil Cytoskeleton.* 1994;29(4):291-300. doi:10.1002/cm.970290402
41. Wu Y, Whiteus C, Xu CS, *et al.* Contacts between the endoplasmic reticulum and other membranes in neurons. *Proc Natl Acad Sci U S A.* Jun 13 2017;114(24):E4859-e4867. doi:10.1073/pnas.1701078114
42. Heiman-Patterson TD, Deitch JS, Blankenhorn EP, *et al.* Background and gender effects on survival in the TgN(SOD1-G93A)1Gur mouse model of ALS. *J Neurol Sci.* Sep 15 2005;236(1-2):1-7. doi:10.1016/j.jns.2005.02.006
43. Trieu VN, Uckun FM. Genistein is neuroprotective in murine models of familial amyotrophic lateral sclerosis and stroke. *Biochem Biophys Res Commun.* May 19 1999;258(3):685-8. doi:10.1006/bbrc.1999.0577
44. Chen D, Wang Y, Chin ER. Activation of the endoplasmic reticulum stress response in skeletal muscle of G93A\*SOD1 amyotrophic lateral sclerosis mice. *Front Cell Neurosci.* 2015;9:170. doi:10.3389/fncel.2015.00170
45. Wegorzewska I, Bell S, Cairns NJ, Miller TM, Baloh RH. TDP-43 mutant transgenic mice develop features of ALS and frontotemporal lobar degeneration. *Proc Natl Acad Sci U S A.* Nov 3 2009;106(44):18809-14. doi:10.1073/pnas.0908767106
46. Xu YF, Gendron TF, Zhang YJ, *et al.* Wild-type human TDP-43 expression causes TDP-43 phosphorylation, mitochondrial aggregation, motor deficits, and early mortality in transgenic mice. *J Neurosci.* Aug 11 2010;30(32):10851-9. doi:10.1523/jneurosci.1630-10.2010
47. Ebstein SY, Yagudayeva I, Shneider NA. Mutant TDP-43 Causes Early-Stage Dose-Dependent Motor Neuron Degeneration in a TARDBP Knockin Mouse Model of ALS. *Cell Rep.* Jan 8 2019;26(2):364-373.e4. doi:10.1016/j.celrep.2018.12.045
48. White MA, Kim E, Duffy A, *et al.* TDP-43 gains function due to perturbed autoregulation in a Tardbp knock-in mouse model of ALS-FTD. *Nat Neurosci.* Apr 2018;21(4):552-563. doi:10.1038/s41593-018-0113-5
49. Brown RH, Al-Chalabi A. Amyotrophic Lateral Sclerosis. *N Engl J Med.* Jul 13 2017;377(2):162-172. doi:10.1056/NEJMr1603471
50. Hardiman O, Al-Chalabi A, Chio A, *et al.* Amyotrophic lateral sclerosis. *Nat Rev Dis Primers.* Oct 5 2017;3:17071. doi:10.1038/nrdp.2017.71
51. Le Pichon CE, Meilandt WJ, Dominguez S, *et al.* Loss of dual leucine zipper kinase signaling is protective in animal models of neurodegenerative disease. *Sci Transl Med.* Aug 16 2017;9(403)doi:10.1126/scitranslmed.aag0394
52. Ghosh R, Wang L, Wang ES, *et al.* Allosteric inhibition of the IRE1alpha RNase preserves cell viability and function during endoplasmic reticulum stress. *Cell.* Jul 31 2014;158(3):534-48. doi:10.1016/j.cell.2014.07.002
53. Morita S, Villalta SA, Feldman HC, *et al.* Targeting ABL-IRE1alpha Signaling Spares ER-Stressed Pancreatic beta Cells to Reverse Autoimmune Diabetes. *Cell Metab.* Apr 4 2017;25(4):883-897.e8. doi:10.1016/j.cmet.2017.03.018
54. Moreno JA, Radford H, Peretti D, *et al.* Sustained translational repression by eIF2 $\alpha$ -P mediates prion neurodegeneration. *Nature.* May 6 2012;485(7399):507-11. doi:10.1038/nature11058

55. Vieira FG, Ping Q, Moreno AJ, *et al.* Guanabenz Treatment Accelerates Disease in a Mutant SOD1 Mouse Model of ALS. *PLoS One.* 2015;10(8):e0135570. doi:10.1371/journal.pone.0135570
56. Moreno JA, Halliday M, Molloy C, *et al.* Oral treatment targeting the unfolded protein response prevents neurodegeneration and clinical disease in prion-infected mice. *Sci Transl Med.* Oct 9 2013;5(206):206ra138. doi:10.1126/scitranslmed.3006767
57. Huttunen HJ, Saarma M. CDFN Protein Therapy in Parkinson's Disease. *Cell Transplant.* Apr 2019;28(4):349-366. doi:10.1177/0963689719840290
58. Hetz C, Chevet E, Oakes SA. Proteostasis control by the unfolded protein response. *Nat Cell Biol.* Jul 2015;17(7):829-38. doi:10.1038/ncb3184
59. Lindahl M, Chalazonitis A, Palm E, *et al.* Cerebral dopamine neurotrophic factor-deficiency leads to degeneration of enteric neurons and altered brain dopamine neuronal function in mice. *Neurobiol Dis.* Feb 2020;134:104696. doi:10.1016/j.nbd.2019.104696
60. Song S, Tan J, Miao Y, Sun Z, Zhang Q. Intermittent-Hypoxia-Induced Autophagy Activation Through the ER-Stress-Related PERK/eIF2 $\alpha$ /ATF4 Pathway is a Protective Response to Pancreatic  $\beta$ -Cell Apoptosis. *Cell Physiol Biochem.* 2018;51(6):2955-2971. doi:10.1159/000496047
61. Song S, Tan J, Miao Y, Zhang Q. Crosstalk of ER stress-mediated autophagy and ER-phagy: Involvement of UPR and the core autophagy machinery. *J Cell Physiol.* May 2018;233(5):3867-3874. doi:10.1002/jcp.26137
62. Nadella R, Voutilainen MH, Saarma M, *et al.* Transient transfection of human CDFN gene reduces the 6-hydroxydopamine-induced neuroinflammation in the rat substantia nigra. *J Neuroinflammation.* Dec 16 2014;11:209. doi:10.1186/s12974-014-0209-0
63. Kovaleva V, Yu L-Y, Ivanova L, *et al.* MANF regulates unfolded protein response and neuronal survival through its ER-located receptor IRE1 $\alpha$ . *bioRxiv.* 2020:2020.09.22.307744. doi:10.1101/2020.09.22.307744
64. Benatar M. Lost in translation: treatment trials in the SOD1 mouse and in human ALS. *Neurobiol Dis.* Apr 2007;26(1):1-13. doi:10.1016/j.nbd.2006.12.015
65. Dafinca R, Barbagallo P, Farrimond L, *et al.* Impairment of Mitochondrial Calcium Buffering Links Mutations in C9ORF72 and TARDBP in iPS-Derived Motor Neurons from Patients with ALS/FTD. *Stem Cell Reports.* May 12 2020;14(5):892-908. doi:10.1016/j.stemcr.2020.03.023
66. Leal SS, Gomes CM. Calcium dysregulation links ALS defective proteins and motor neuron selective vulnerability. *Front Cell Neurosci.* 2015;9:225. doi:10.3389/fncel.2015.00225
67. Tedeschi V, Petrozziello T, Secondo A. Calcium Dyshomeostasis and Lysosomal Ca(2+) Dysfunction in Amyotrophic Lateral Sclerosis. *Cells.* Oct 8 2019;8(10)doi:10.3390/cells8101216
68. Kieran D, Woods I, Villunger A, Strasser A, Prehn JH. Deletion of the BH3-only protein puma protects motoneurons from ER stress-induced apoptosis and delays motoneuron loss in ALS mice. *Proc Natl Acad Sci U S A.* Dec 18 2007;104(51):20606-11. doi:10.1073/pnas.0707906105
69. Chen S, Liao Q, Lu K, Zhou J, Huang C, Bi F. Riluzole Exhibits No Therapeutic Efficacy On a Transgenic Rat model of Amyotrophic Lateral Sclerosis. *Curr Neurovasc Res.* Apr 9 2020;doi:10.2174/1567202617666200409125227
70. Gurney ME, Cutting FB, Zhai P, *et al.* Benefit of vitamin E, riluzole, and gabapentin in a transgenic model of familial amyotrophic lateral sclerosis. *Ann Neurol.* Feb 1996;39(2):147-57. doi:10.1002/ana.410390203



71. Ito H, Wate R, Zhang J, *et al.* Treatment with edaravone, initiated at symptom onset, slows motor decline and decreases SOD1 deposition in ALS mice. *Exp Neurol.* Oct 2008;213(2):448-55. doi:10.1016/j.expneurol.2008.07.017

## Figure legends

**Figure 1 Continuous i.c.v infusion of CDNF improves motor behavior and protects spinal MNs in the ChAT-tTA/TRE-TDP43-M337V rat model.** (A) Experimental design: upon reaching adult age, Alzet minipumps connected to a catheter were implanted in ChAT-tTA/TRE-TDP43-M337V and tTA rats to infuse CDNF (6 µg/day) or PBS. One week later, the activation of transgene was induced by partial withdrawal of Dox. Rats were monitored for weight and motor behavior changes until day 21 from transgene induction, when the rats were perfused. (B) Latency to fall of PBS/CDNF-treated transgenic and tTA littermates recorded three times per week. BL=baseline. (C) Quantification and comparison of the number of MNs in the lumbar (L) spinal cord, area L3-L5. (D) Representative images of Nissl and ChAT<sup>+</sup> MNs in the lumbar spinal cord. Scale bar 500 µm. Mean ± SEM, *n*=4-9/group in **B-D**. \**P*<0.05, \*\**P*<0.01, \*\*\*\**P*<0.0001, repeated measures ANOVA followed by Tukey post-hoc test in **B** and one-way ANOVA followed by Tukey post-hoc test in **C**.

**Figure 2 CDNF treatment decreases UPR markers expression in TDP43-M337V expressing MNs.** (A) Effect of CDNF alone or in combination with different concentrations of 4µ8C, KIRA6 or GSK2606414 on MNs survival after 24h of thapsigargin (5 nM) treatment. Mean ± SEM of at least 3 different experiments. (B) Percentage of MNs survival 5 days after treatment with different concentrations of IRE1 inhibitors 4µ8C and KIRA6 and PERK inhibitor GSK2606414. The effect of the inhibitors was evaluated either in presence or absence of trophic factor CNTF and BDNF. Mean ± SEM of 3 different experiments (C) Effect of CDNF on the clustering of IRE1-3FH5GFP in MNs treated with TP. (D) Effect of CDNF on ATF6 translocation from cytoplasm to nucleus in MNs treated with TP. (E) Quantification of the number of IRE1-3FH5GFP per cell in **C**. (F) Quantification of the percentage of cells with IRE1-3FH5GFP clusters in **C**. Mean ± SEM of 5 different experiments in **C**, **E** & **F**. At least 15 cells per experiment were analysed. (G) Quantification of **D**. Mean ± SEM of at least 45 cells from

three different experiment. **(H-J)** Protein expression of UPR markers phosphorylated eIF2 $\alpha$  and CHOP in the MNs expressing TDP43 WT and TDP43-M337V, which were previously stressed with TP and TM. **(K)** Representative blots of p-eIF2 $\alpha$  and CHOP. Mean  $\pm$  SEM of 5 different experiments in **H-J**. \* $P$ <0.05, \*\* $P$ <0.01, \*\*\* $P$ <0.001; one way ANOVA followed by Tukey post-hoc test in **A-B**; two-way ANOVA followed by Sidak post-hoc test in **E-J**.

**Figure 3 CDNF administration attenuates the expression of UPR markers in the spinal cord of ChAT-tTA/TRE-TDP43-M337V rats at 21 days after transgene activation.** **(A)** Representative fluorescence images of ChAT (Green) and GRP78 (Red) protein expression in PBS/CDNF-treated ChAT-tTA/TRE-TDP43-M337V compared to PBS/CDNF-treated tTA rats. Scale bar 50  $\mu$ m. **(B)** Quantification of the pixel value of GRP78 in the lumbar ventral horn area. **(C)** Quantification of the pixel value of GRP78 in the ChAT<sup>+</sup> MNs. Mean  $\pm$  SEM,  $n=5-9$ /group. **(D)** Representative fluorescence images of ChAT (Green) and p-eIF2 $\alpha$  (Red) protein expression in PBS/CDNF-treated ChAT-tTA/TRE-TDP43-M337V compared to PBS/CDNF-treated tTA rats. Scale bar 50  $\mu$ m. **(E)** Quantification of the pixel value of p-eIF2 $\alpha$  in the lumbar ventral horn area. **(F)** Quantification of the pixel value of p-eIF2 $\alpha$  in the ChAT<sup>+</sup> MNs. Mean  $\pm$  SEM,  $n=5-9$ /group; \* $P$ <0.05, \*\*\* $P$ <0.001, \*\*\*\* $P$ <0.0001; one-way ANOVA followed by Tukey post-hoc test in **B, C, E** and **F**.

**Figure 4 A single i.c.v. injection of CDNF halts disease progression, ameliorates motor behavior, and improves the survival of mice and spinal MNs in the SOD1-G93A mouse model.** **(A)** SOD1 mice with early disease signs and WT littermates were injected with 10  $\mu$ g of CDNF or vehicle at 13 weeks of age. Animals were monitored twice per week for weight changes, disease development, and motor performance. **(B-C)** Survival of SOD1-G93A mice upon a single injection of CDNF or PBS treatment. The median survival time in females was 148 days for CDNF-treated mice and 140 days for PBS-treated mice. Therefore, there was an increase of 8 days. In the males, the median survival was 140.5 days for the CDNF-treated mice and 132 days for the PBS-treated mice. The increase was 8.5 days. **(D-E)** Latency to fall of CDNF/PBS treated-SOD1-G93A and WT littermates measured every week. **(F-G)** Travel time of CDNF or PBS-treated SOD1-G93A mice along suspended rods of decreasing diameters (27 to

8 mm) one week after treatment. **(H)** Number of rearings of CDNF/PBS treated-SOD1-G93A and WT littermates in the open field paradigm measured at 1 and 3 weeks after injection. **(I)** Quantification and comparison of the number of MNs in the lumbar spinal cord after CDNF or vehicle treatment. Mean  $\pm$  SEM,  $n=10-12$ /group in **B-C**,  $n=18-20$  for females,  $n=14-15$  for males,  $n=20$  for WT in **D-G**,  $n=11$ /group in **H**,  $n=3$  for WT and  $n=5$  for SOD1 in **I**. \* $P<0.05$ , \*\* $P<0.01$ , \*\*\* $P<0.001$ , \*\*\*\* $P<0.0001$ , log-rank test in **B-C**, repeated measures ANOVA followed by Tukey post-hoc test in **D-E** and **H**; unpaired t-test in **F-G**; one-way ANOVA followed by Tukey post-hoc in **I**.

**Figure 5 CDNF protein administration increases the survival of SOD1-G93A mouse-derived embryonic MNs and reduces the expression of UPR markers after toxin treatment.**

**(A)** Survival of WT and SOD1-G93A embryonic MNs upon CDNF or CNTF and BDNF treatment. **(B)** Effect of CDNF administration on WT and SOD1 MNs survival upon 5 nM thapsigargin (TP) treatment or no treatment. **(C)** Dose-response curve of CDNF administration upon TP treatment on WT and SOD1-G93A MNs survival. **(D)** Effect of CDNF on ATF6 translocation from cytoplasm to nucleus in MNs treated with TP or tunicamycin (TM). **(E)** Quantification of **D**, each dot representing the ratio of an individual cell. **(F)** mRNA expression of UPR markers *Xbp1s* in the MNs treated as in Figure **B**. **(G-H)** Expression levels of eIF2 $\alpha$  phosphorylation and CHOP protein, respectively, in the MNs treated as in Figure **D**. **(I)** Representative blots for the quantification in **G** and **H**. Mean  $\pm$  SEM of 3 independent experiments in **A**, **B**, **C** (18-33 cells) and **F**, 4 and 7 experiments in **G-I**. \* $P<0.05$ , \*\* $P<0.01$ , \*\*\* $P<0.001$ , two-way ANOVA followed by Bonferroni post-hoc test in **B** and **F**, and Sidak's post-hoc test in **C**, **E**, **G** and **H**. TG=transgenic.

**Figure 6 A single i.c.v. injection of CDNF decreases the expression of UPR markers in the lumbar spinal cord of SOD1-G93A animals at 17 weeks.**

**(A)** Representative pictures of a lumbar spinal cord section before and after the MNs dissection and mRNA level of *Chat*, marker of spinal cord MNs, in the putative MNs area and in a control region where no MNs should be present (marked with \*). **(B-F)** mRNA expression of UPR markers *Atf6*, *Atf4*, *Chop*, *Xbp1t* and *Xbp1s* in microdissected lumbar MNs after CDNF/PBS injection in 13 and 17 weeks

SOD1-G93A mice and WT littermates. **(G)** Expression of GRP78 protein in lumbar MNs after CDNF/PBS treatment in 17 weeks SOD1-G93A mice and WT littermates. **(H)** Quantification of **G**. **(I)** Expression of p-eIF2 $\alpha$  protein in lumbar MNs after CDNF/PBS treatment in 17 weeks SOD1-G93A mice and WT littermates. **(J)** Quantification of **I**. Mean  $\pm$  SEM,  $n=6-9$ /group in **B-F**,  $n=3-5$ /group in **G-J**. \* $P<0.05$ , \*\* $P<0.01$ , \*\*\*\* $P<0.0001$ , # $P<0.05$ , ## $P<0.01$ , ### $P<0.001$ , two-way ANOVA followed by Bonferroni post-hoc test in **B-F**, one-way ANOVA followed by Tukey post-hoc test in **H** and **J**.

**Figure 7 CDNF treatment decreases UPR markers expression in a novel TDP43-M337V mouse model with ER stress pathology.**

**(A)** Schematic representation of the appearance of ER stress and MNs loss in the novel TDP43-M337V mouse model. **(B)** TDP43-M337V mice were injected at 6 weeks of age and UPR markers were analysed by qPCR at 6 months. **(C-H)** mRNA expression of UPR markers *Atf6*, *Atf4*, *Chop*, *Xbp1t*, *Xbp1s* and *Grp78* in micro-dissected lumbar MNs from 6 months TDP43-M337V mice treated with CDNF or vehicle at 6 weeks of age. **(I)** mRNA expression of UPR markers *Atf6*, *Chop*, *Xbp1s* and *Grp78* in total lysates of motor cortex from 6 months TDP43-M337V mice treated with CDNF or vehicle at 6 weeks of age; results are presented as fold change increase compared to naïve control. Mean  $\pm$  SEM,  $n=5/6$ /group in **C-H**,  $n=5$ /group in **I**. \* $P<0.05$ , \*\* $P<0.01$ ; two-way ANOVA followed by Bonferroni post-hoc test in **C-H**; unpaired t-test in **I**.

**Figure 8 CDNF rescues MNs and improve motor performance in 18 months old TDP43-M377V mice.**

**(A)** Experimental timeline: injected mice were monitored for weight changes and motor performance once per week. The mice were sacrificed 5 weeks after CDNF/PBS administration and the spinal cord was collected for immunohistochemistry. **(B-E)** Latency to fall in a rotarod test with rocking and reverse acceleration in WT females **(B)**, WT males **(C)**, TDP43-M337V females **(D)**, and TDP43-M337V males **(E)**. **(F)** Quantification of the number of Chat and Nissl<sup>+</sup> in the lumbar (L) spinal cord, area L3-L5, of WT and TDP43-M337V mice. **(G)** Representative images of Nissl and ChAT<sup>+</sup> MNs in the lumbar spinal cords. Scale bar 500  $\mu$ m. Mean  $\pm$  SEM,  $n=8$ /group for females,  $n=5-6$ /group for males,  $n=4-6$ /group for WT in **B-E**,  $n=13-14$ /group for TDP43-M337V mice and  $n=9-10$  for WT mice in **F**. \* $P<0.05$ , \*\* $P<0.01$ ,

\*\*\* $P < 0.001$ , \*\*\*\* $P < 0.0001$ , Kruskal-Wallis test followed by Dunn's Multiple Comparisons test in **B-E**, one-way ANOVA followed by Tukey post-hoc test in **F**.

ACCEPTED MANUSCRIPT

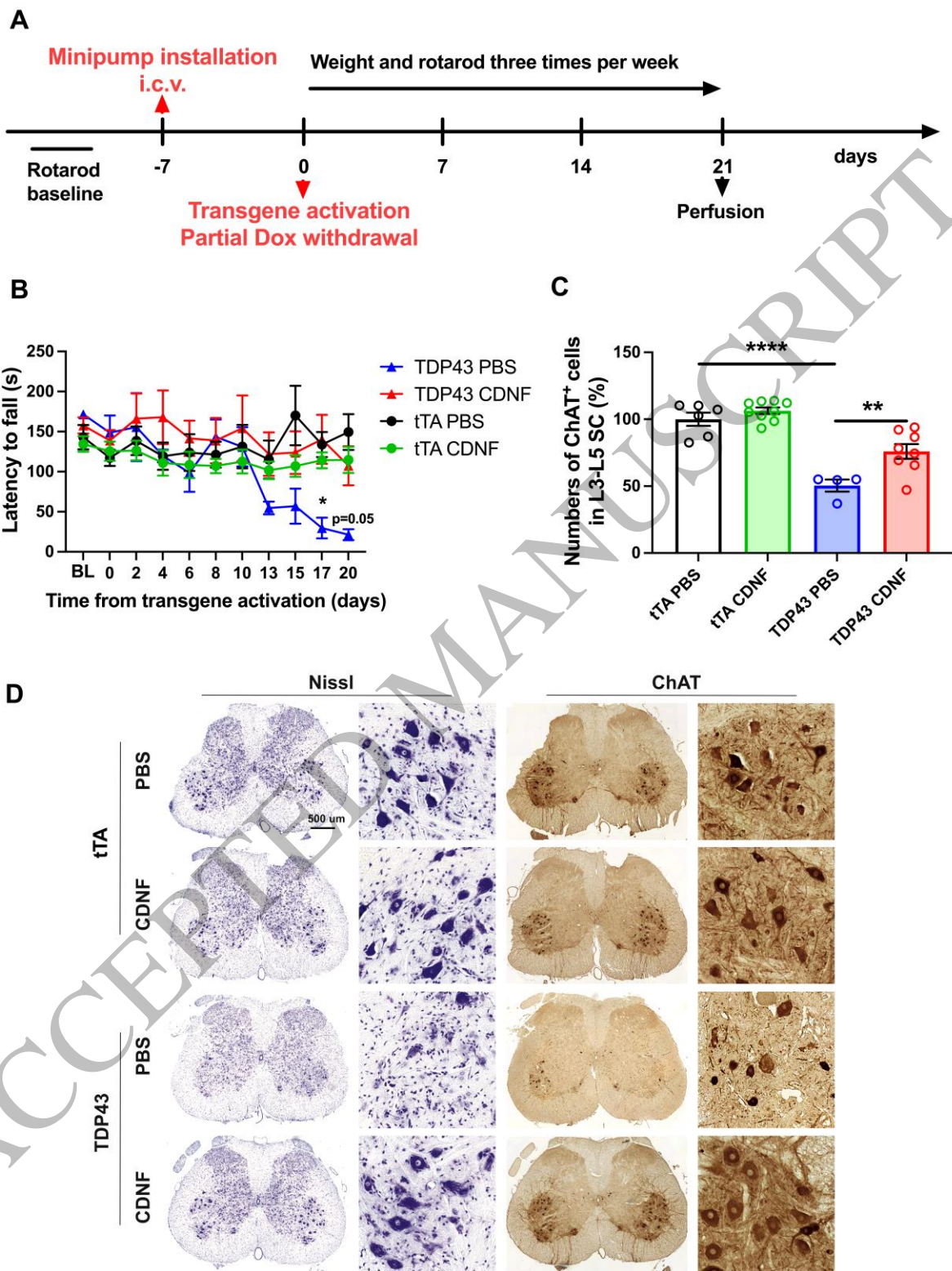
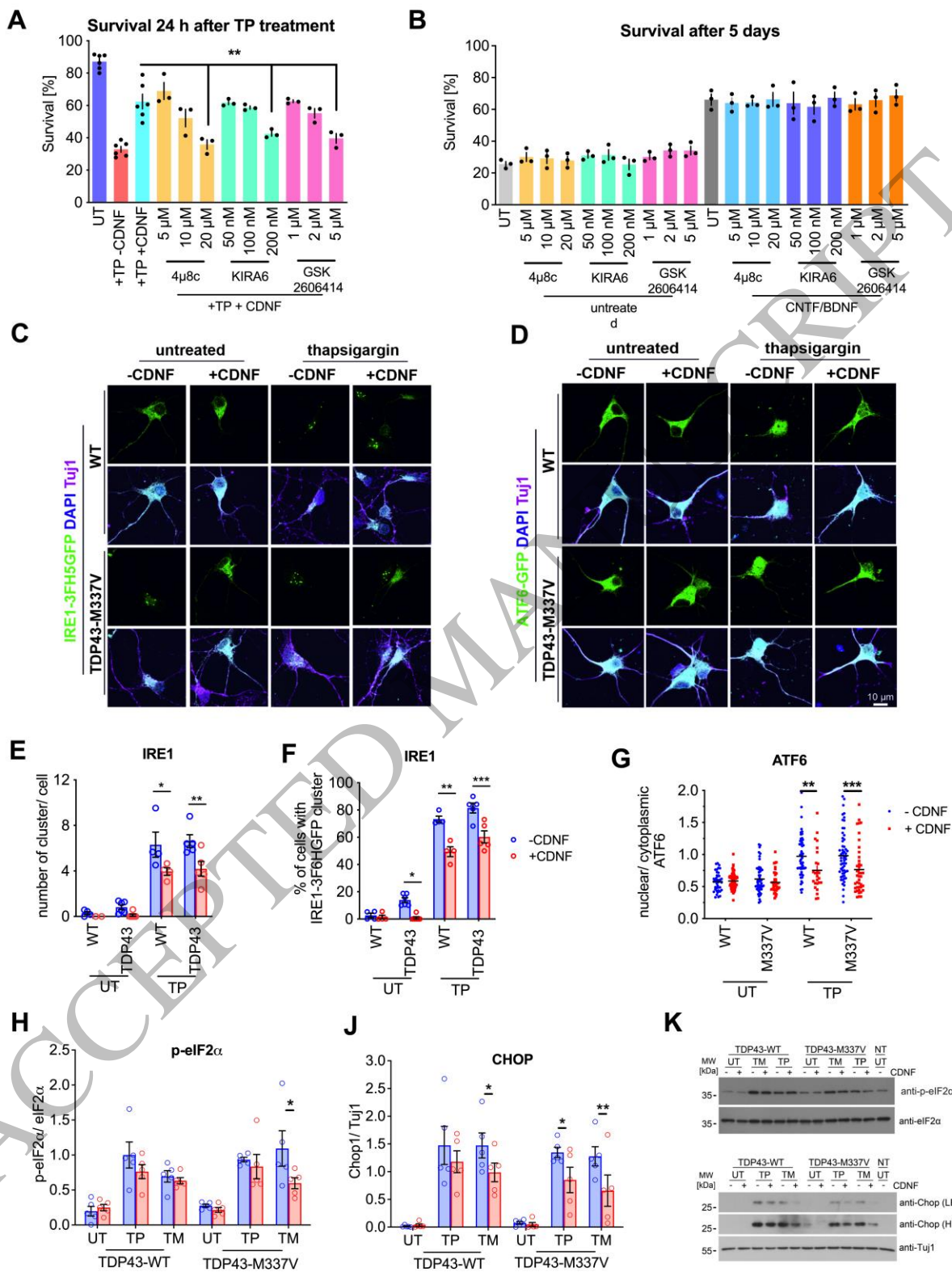


Figure 1  
159x207 mm (.21 x DPI)



**Figure 2**  
159x211 mm (.21 x DPI)

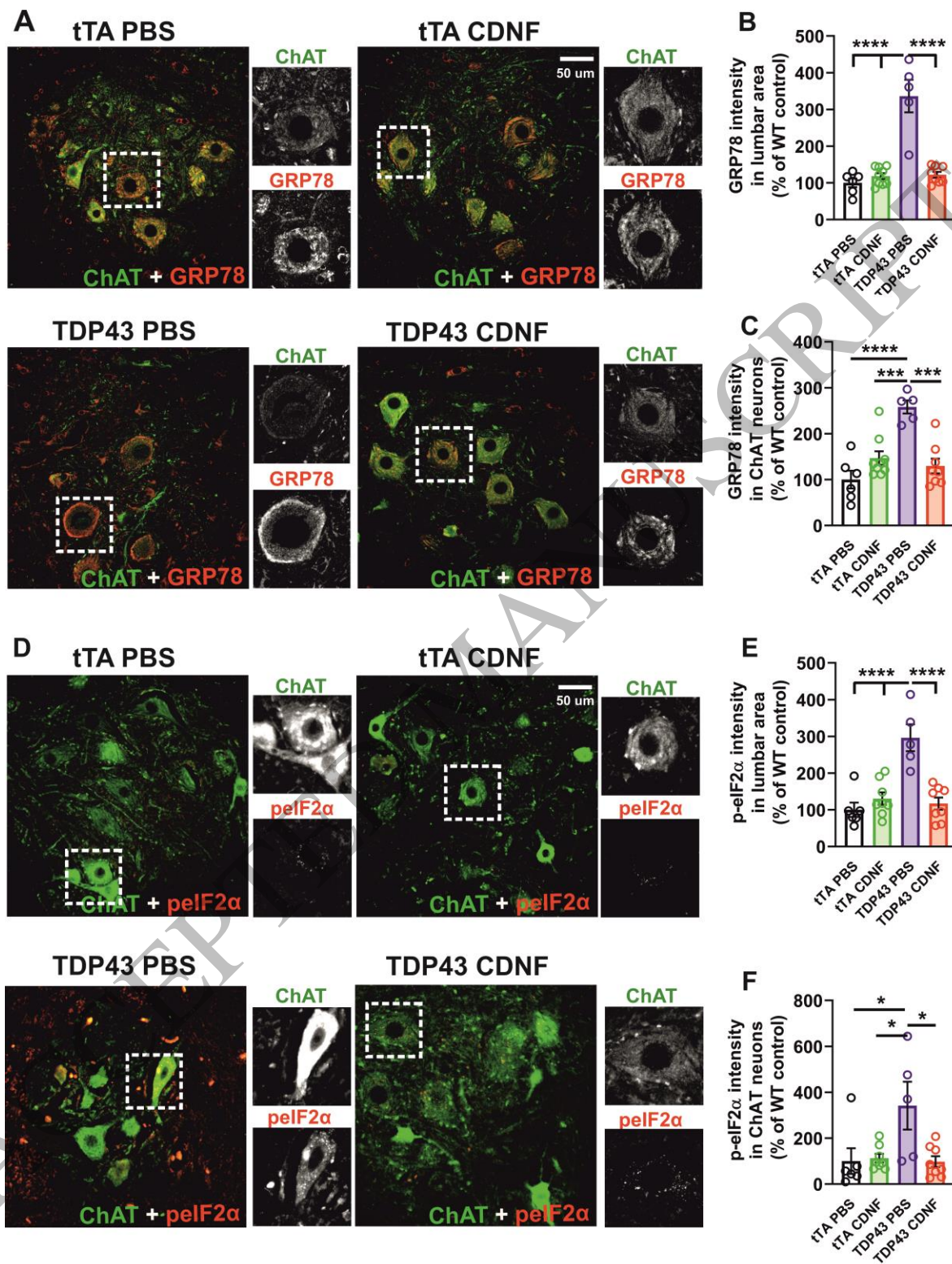


Figure 3  
159x205 mm (.21 x DPI)



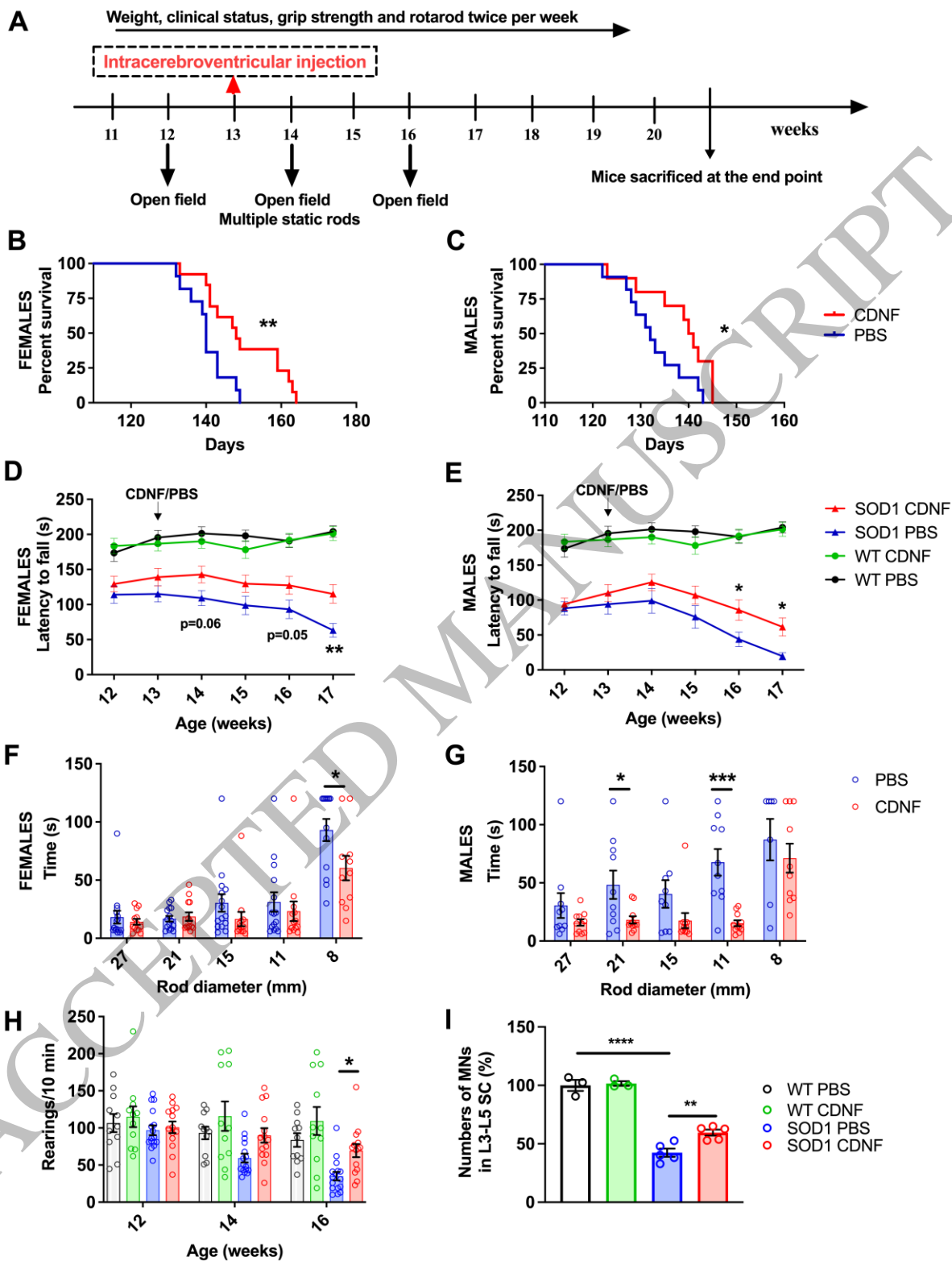


Figure 4  
159x210 mm (.21 x DPI)

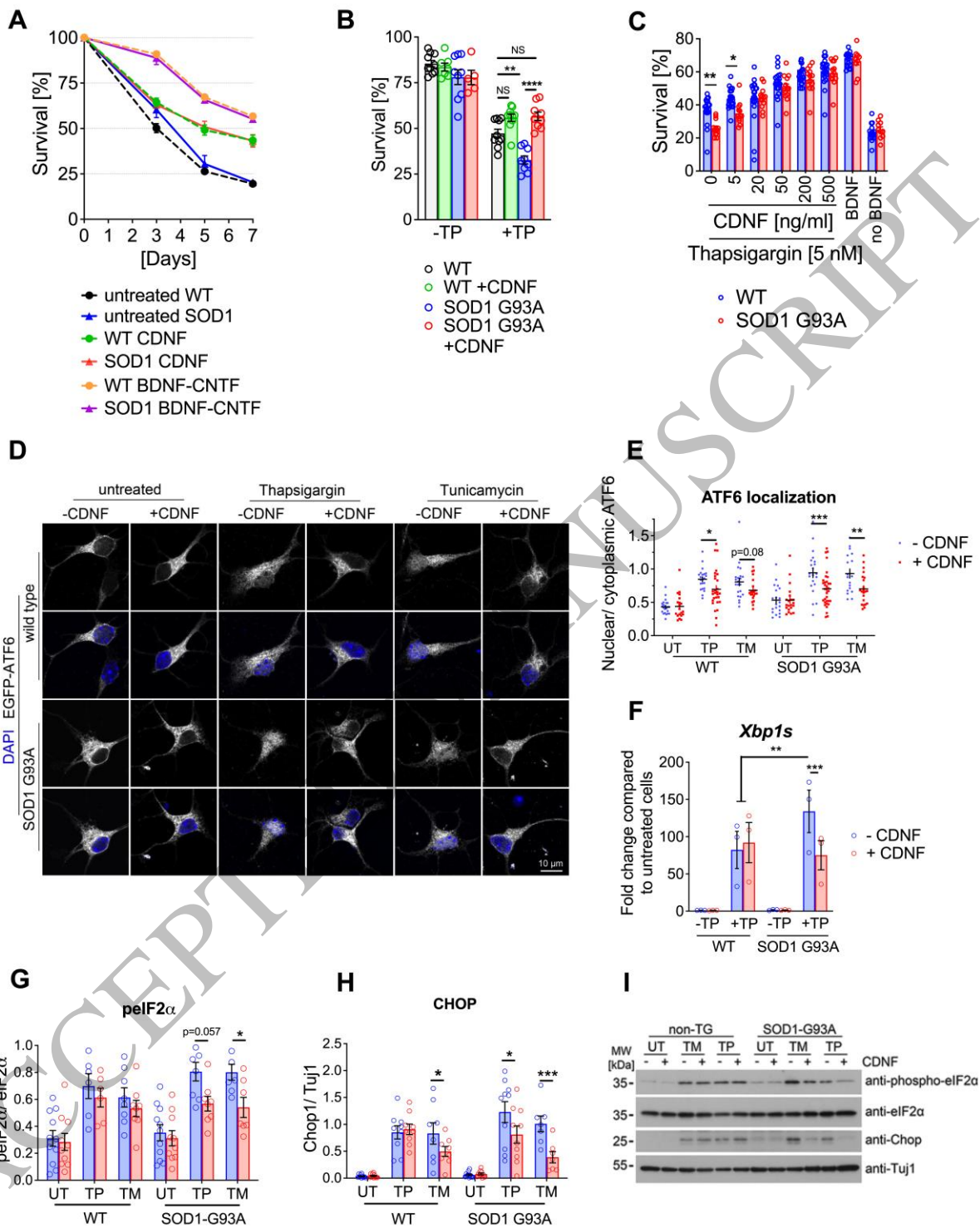


Figure 5  
159x197 mm (.21 x DPI)

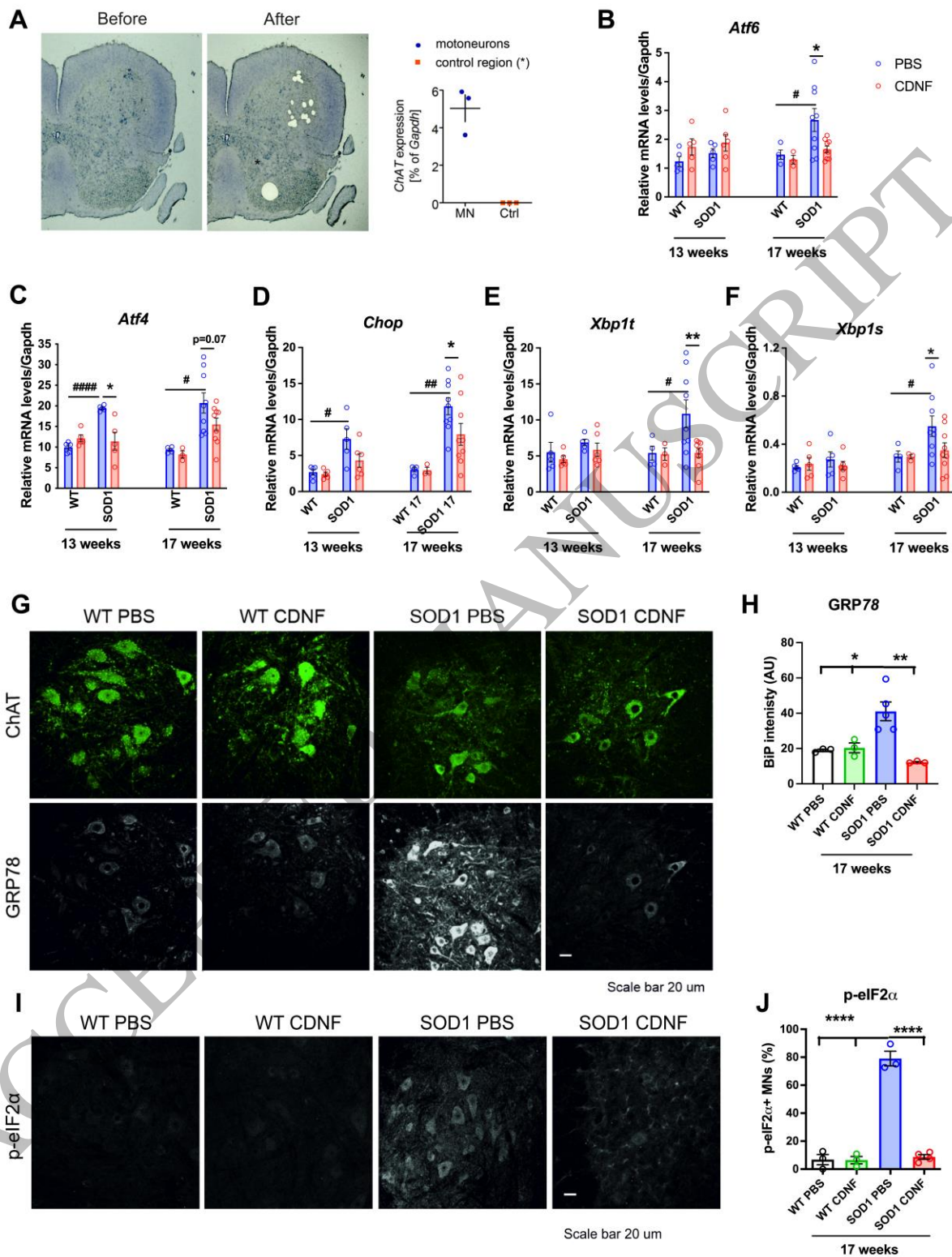


Figure 6  
159x207 mm (.21 x DPI)

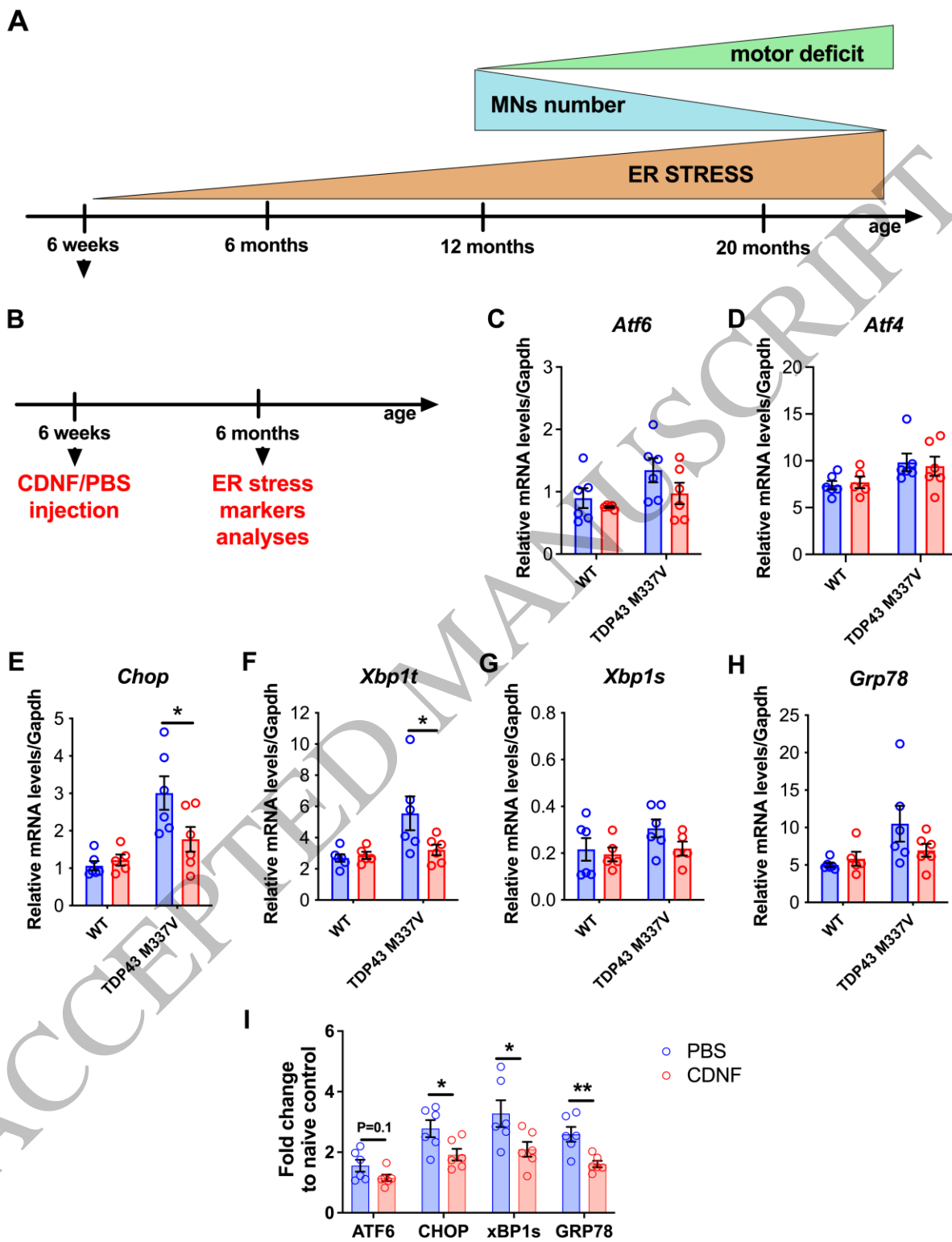


Figure 7  
159x206 mm (.21 x DPI)

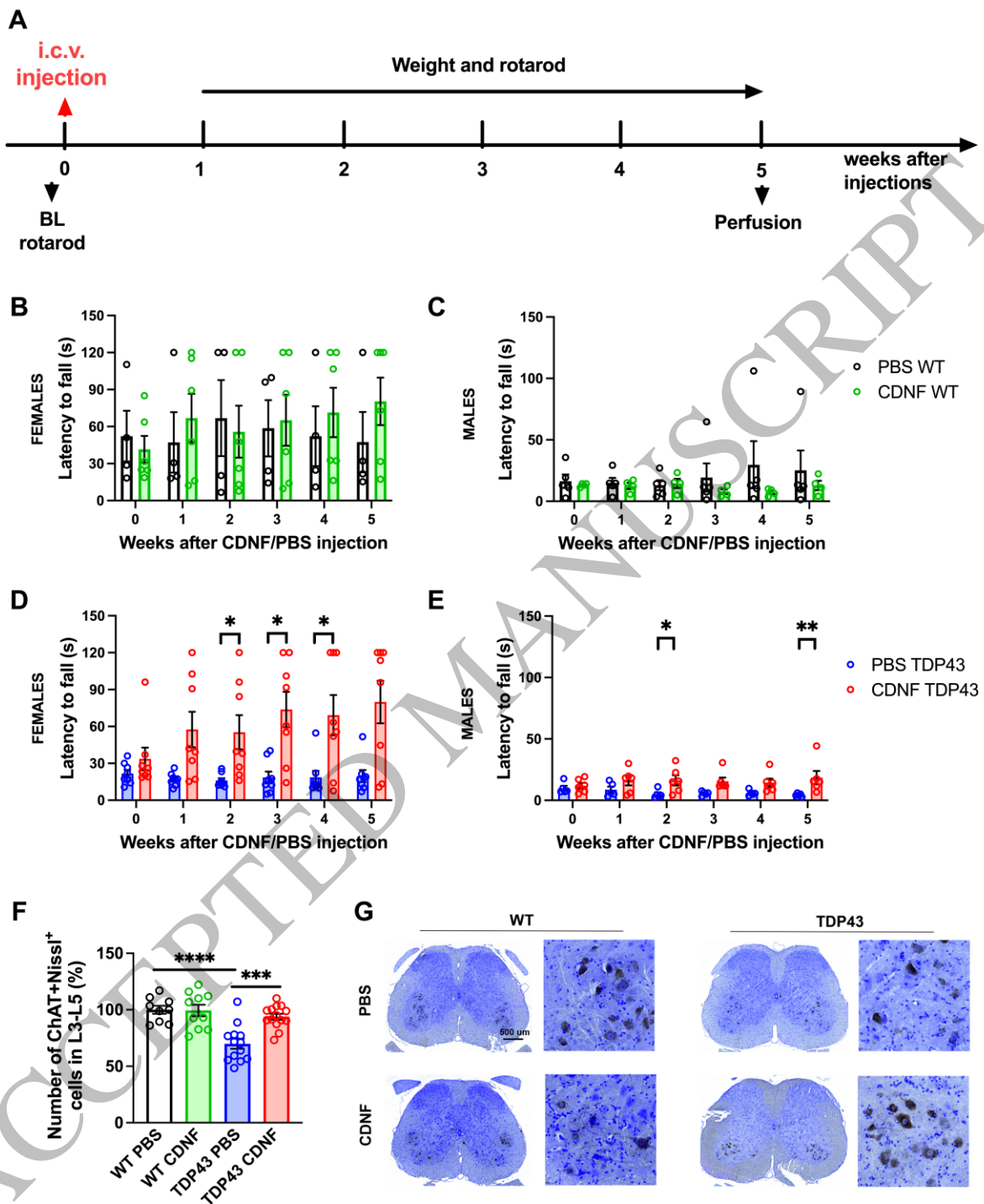


Figure 8  
159x193 mm (.21 x DPI)